

Janus-type dendrimers based on highly branched fluorinated chains with tunable self-assembly and ^{19}F nuclear magnetic resonance properties

Marta Rosati,[†] Angela Acocella,[◇] Andrea Pizzi,[†] Giorgio Turtu,[◇] Giulia Neri,[†] Nicola Demitri,[§] Nonappa,[‡] Giuseppina Raffaini,[#] Bertrand Donnio,[‡] Francesco Zerbetto,[◇] Francesca Baldelli Bombelli,^{*,†} Gabriella Cavallo,^{*,†} Pierangelo Metrangolo^{*,†}

[†] Laboratory of Supramolecular and Bio-Nanomaterials (SupraBioNanoLab), Department of Chemistry, Materials, and Chemical Engineering “Giulio Natta”, Politecnico di Milano, Via Luigi Mancinelli 7, Milan, Italy. E-mail: francesca.baldelli@polimi.it; gabriella.cavallo@polimi.it; pierangelo.metrangolo@polimi.it.

[§] Elettra – Sincrotrone Trieste, S.S. 14 Km 163.5 in Area Science Park, 34149 Basovizza – Trieste, Italy.

[‡] Faculty of Engineering and Natural Sciences, Tampere University, FI-33720, Tampere, Finland.

[#] Department of Chemistry, Materials, and Chemical Engineering “Giulio Natta”, Politecnico di Milano, Via Luigi Mancinelli 7, Milan, Italy.

[‡] Institut de Physique et Chimie des Matériaux de Strasbourg – IPCMS, UMR 7504 – CNRS/ Université de Strasbourg, F-67034 Strasbourg Cedex 2, France.

[◇] Alma Mater Studiorum - Università di Bologna, Dipartimento di Chimica “G. Ciamician”, Via F. Selmi, 2, 40126 Bologna, Italy.

KEYWORDS

Fluorine, ^{19}F -NMR, dendrimers, self-assembly, dendrimersomes, coarse-grain simulations.

Supporting Information

Table of contents:

- **General information**
- **Synthesis of the azide terminating derivative of the fluorinated pentaerythritol (F₂₇-N₃)**
- **Synthesis of FJD₁, FJD₂, and FJD₃: Convergent-like approach**
- **Synthesis of FJD₁, FJD₂, and FJD₃: Divergent-like approach**
- **Single Crystal X-Ray Diffraction**
- **Thermal analysis and SWAXS characterization**
- **Self-assembly in solution**
- **AA-MD simulations details**
- **AA-MD dimer simulations conformational analysis**
- **Coarse-grain simulations details**
- **Snapshots of morphologies of aggregates forming in pure water with 40rc x 40rc x 40rc simulation box.**
- **Figures**

- **General information**

For the synthesis the employed chemicals as reactants and solvents were used as received without further purification and purchased with purity >97% from: ©TCI Deutschland GmbH; Sigma Aldrich, Germany; Fluorochem, UK.

Thin layer chromatography TLC was conducted on plates precoated with silica gel Si 60-F254 (Merck, Darmstadt, Germany).

Flash chromatography was carried out on J. T. Baker silica gel mesh size 230–400.

Nuclear Magnetic Resonance spectroscopy (NMR)

All the NMR spectra were recorded on a Bruker AV400 Bruker AvanceIII 400 MHz spectrometer equipped with a 5 mm QNP probe (^{19}F , ^{31}P - ^{13}C / ^1H). NMR spectra were recorded at $(300 \pm 3 \text{ K})$ and chemical shifts are reported in ppm downfield from SiMe_4 with the residual proton (CHCl_3 $d=7.26$ ppm, CD_3OD : $d=3.31$ ppm) and carbon (CDCl_3 : $d=77.0$ ppm, CD_3OD : $d=49$ ppm). Proton and carbon assignments were achieved by means of ^{13}C -APT, ^1H - ^1H COSY, and ^1H - ^{13}C HSQC experiments. Coupling constant values, J , are given in Hz.

Data evaluation was done with MestreNova 10.0 from Mestre-Lab. The samples prepared for the characterization of the compound synthesized were prepared by dissolving 5-10mg in 500 μL of the deuterated solvent. Methanol- d_4 (99 atom % D) and Chloroform- d , 99.8 atom % D were purchased from Sigma Aldrich, Germany.

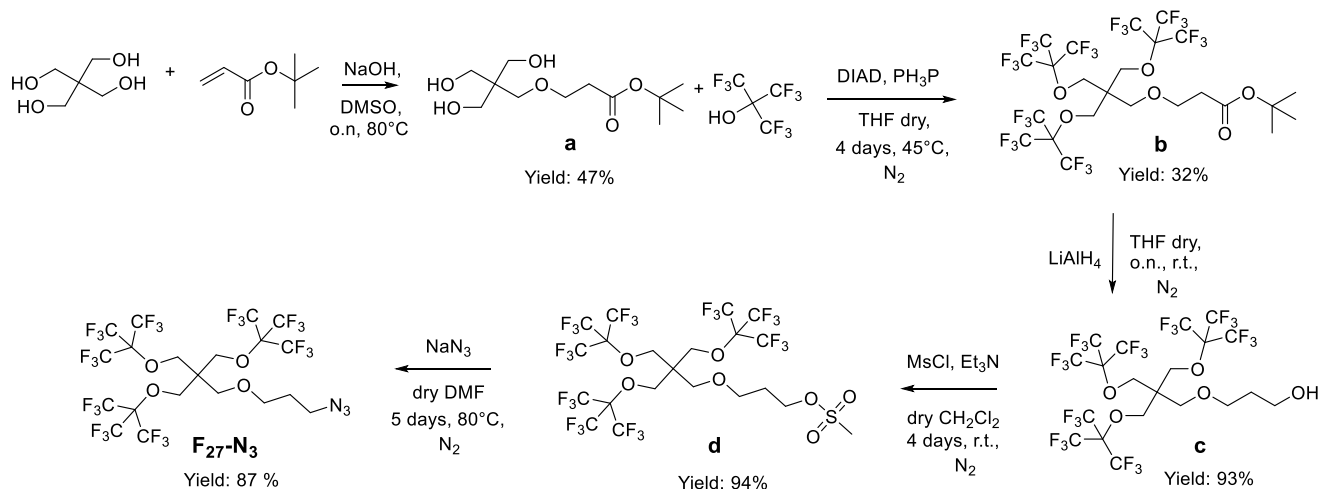
Attenuated Total Reflection Fourier-Transform Infrared spectroscopy (FTIR)

FTIR was measured with a Thermo Scientific Nicolet iS50 FTIR spectrometer, equipped with iS50 ATR accessory (Thermo Scientific, Madison, USA). IR signal values were expressed in wavenumber (cm^{-1}) and rounded to the nearest whole number through automatic assignment using OMNICTM IR software. Air was recorded as background. The analysis was made in transmittance mode in a wavenumber window of 4000-400 cm^{-1} .

Elemental analysis was done by Redox Srl, in Monza (MB), Italy.

High resolution ESI Mass spectrometry was done by UNITECH COSPECT: Comprehensive Substances characterization via advanced spectroscopy Via C. Golgi 19, University of Milan

• **Synthesis of the azide terminating derivative of the fluorinated pentaerythritol (F₂₇-N₃)**



Scheme S1: Synthesis of the F₂₇-N₃ derivative: the synthesis of compounds **a** to **d** has been done following already reported procedure^[S1, S2].

Compounds **a** to **d** were prepared according to procedures previously reported in literature^[S1, S2].

Compound a. Pentaerythritol (100 g, 1 equivalent) was dissolved in 200 mL of dimethyl sulfoxide; then a solution of NaOH (40g, 0.2 equivalents) in 15 mL of deionized water was added at 0 °C followed by the addition of tert-butyl acrylate (128 mL, 1.2 equivalents). The reaction was run stirring at 80 °C overnight. A 2 M hydrochloric acid solution was added till reaching an acidic pH. Then, an extraction was made with ethyl acetate. The crude was purified by silica gel flash chromatography using as eluent a mixture of diethyl ether and acetone (1:1) (R_f = 0.3). The compound is isolated as an oil. (Yield: 47%)

¹H NMR (400 MHz, Chloroform-*d*) δ 3.67 (t, *J* = 5.9 Hz, 2H), 3.65 (s, 6H), 3.51 (s, 2H), 2.47 (t, *J* = 5.8 Hz, 2H), 1.45 (s, 9H).

Compound b. Compound **a** (1.363 g; 1 equivalent) and triphenyl phosphine (PPh₃) (8.12 g, 6 equivalents) were dissolved in 38 mL of anhydrous THF. Then, diisopropyl azodicarboxylate (DIAD) (6.1 mL, 6 equivalents) was slowly added to the reaction mixture at 0 °C. The mixture was left in stirring and nitrogen atmosphere till precipitation of the adduct. Then, perfluoro-*tert*-butyl alcohol (4 mL, 6 equivalents) was added. The reaction was run at 45 °C, in stirring and nitrogen atmosphere for four days. Then, the reaction mixture was extracted from water with dichloromethane, the organic phase was dried with Na₂SO₄, and filtered. After the removal of the solvent, the mixture was recrystallized in Methanol. The product is collected as a white crystalline solid. (Yield: 53%).

¹H NMR (400 MHz, Chloroform-*d*) δ 4.05 (s, 6H), 3.64 (t, *J* = 6.5 Hz, 2H), 3.43 (s, 2H), 2.44 (t, *J* = 6.5 Hz, 2H), 1.44 (s, 9H). ¹⁹F NMR (376 MHz, CDCl₃) δ -70.45.

Compound c. Lithium aluminium hydride (0.4g, 4 equivalents) was put in nitrogen atmosphere and is dispersed in 50 mL of anhydrous THF at 0 °C. Then, compound **b** (1.363 g; 1 equivalent) was slowly added to the reaction

mixture at 0 °C. The reaction was run at room temperature, in stirring and nitrogen atmosphere overnight. Then, then the reaction mixture was filtered and the volume of THF was reduced by rotary evaporation. Afterward, an extraction from water with dichloromethane was done, the organic phase was dried with Na₂SO₄ and filtered. After the removal of the solvent, the product was collected as an uncoloured oil. (Yield: 93%).

¹H NMR (400 MHz, Chloroform-*d*) δ 4.05 (s, 6H), 3.72 (t, *J* = 6.2 Hz, 2H), 3.53 (t, *J* = 6.1 Hz, 2H), 3.40 (s, 2H), 1.82 (p, *J* = 6.2 Hz, 2H). ¹⁹F NMR (376 MHz, CDCl₃) δ -70.43.

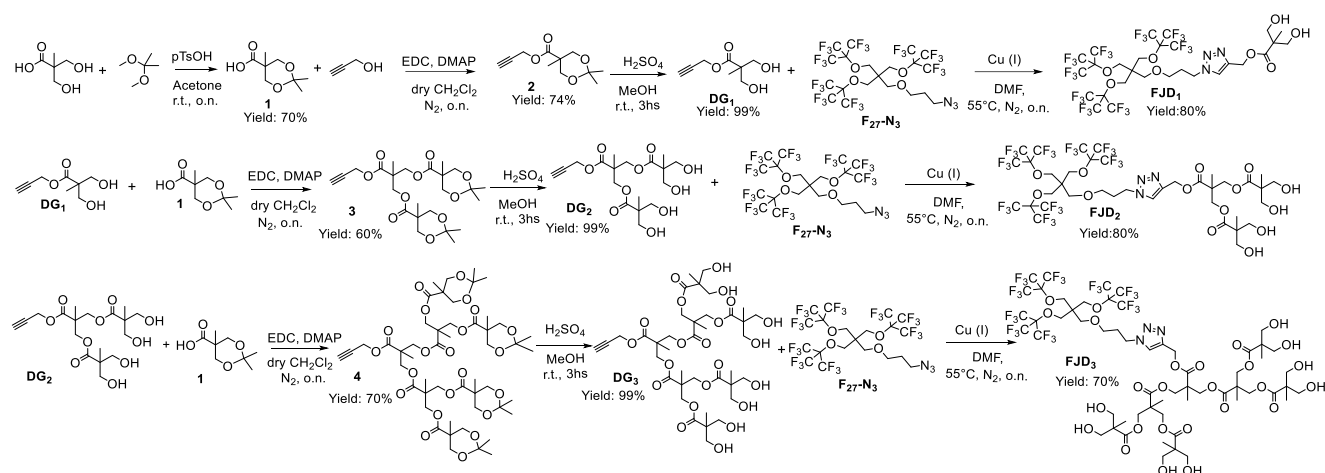
Compound d. Compound **c** (0.85 g; 1 equivalent) was dissolved in 26 mL of anhydrous dichloromethane. Then, triethyl amine (0.9 mL, 3 equivalents) and methanesulfonyl chloride (MsCl) (0.52 mL, 3 equivalents) were added to the reaction mixture. The reaction was run at room temperature, in stirring and nitrogen atmosphere for four days. Then, the reaction mixture was extracted from water with dichloromethane, the organic phase was dried with Na₂SO₄, and filtered. After the removal of the solvent, the product was left in vacuum to remove all the excess of solvents. The product was collected as a pale-yellow oil. (Yield: 94%).

¹H NMR (400 MHz, Chloroform-*d*) δ 4.27 (t, *J* = 6.3 Hz, 2H), 4.05 (s, 6H), 3.52 (t, *J* = 6.1 Hz, 2H), 3.41 (s, 2H), 2.99 (s, 3H), 2.00 (p, *J* = 6.2 Hz, 2H). ¹⁹F NMR (376 MHz, CDCl₃) δ -70.41.

F₂₇-N₃. Compound **d** (2.9 g; 1 equivalent) was dissolved in 19 mL of dry DMF at room temperature, under N₂ atmosphere and stirring. Then, sodium azide (0.454 g; 2.2 equivalents) was added. The reaction was run at 80 °C under inert atmosphere for 5 days (to control the progress of the reaction 200 μL of the solution were collected and analyzed by ¹H-NMR). The reaction mixture was run at room temperature, added to iced water and extracted with Hexane. The organic phase was dried with NaSO₄ and the solvent was removed through rotary evaporation. The product was obtained as an uncoloured oil (Yield: 87%).

¹H NMR (400 MHz, Chloroform-*d*) δ 4.27 (t, *J* = 6.3 Hz, 2H), 4.05 (s, 6H), 3.52 (t, *J* = 6.1 Hz, 2H), 3.41 (s, 2H), 2.99 (s, 3H), 2.00 (p, *J* = 6.2 Hz, 2H). ¹³C NMR (101 MHz, Chloroform-*d*) δ 120.31 (q, ¹*J*_{C-F} = 292.7 Hz), 79.85 (m, ²*J*_{C-F} = 29.9 Hz), 68.52, 66.22, 65.61, 48.42, 46.37, 28.98. ¹⁹F NMR (376 MHz, Chloroform-*d*) δ -70.44. ATR-FTIR: Stretching C-H: 2962-2850 cm⁻¹; Stretching N=N=N: 2105 cm⁻¹; Stretching C-F: 1350 cm⁻¹; Bending C-F: 700 cm⁻¹. El. Analysis % Calculated for C₂₀H₁₄F₂₇N₃O₄: theoretical C, 27.51; H, 1.62; F, 58.74; N, 4.81; O, 7.33/ Found C, 27.23; H, 1.67; N, 4.76; F, 58.03; O, 8.31.

• **Synthesis of FJD₁, FJD₂, and FJD₃: Convergent-like approach**



Scheme S2: Synthesis of the Janus dendrimers FJD₁₋₃: convergent-like approach.

Compound 1. Bis-MPA (5 g; 1 equivalent) and para-toluensulfonic acid (0.520 g; 0.1 equivalents) were put in nitrogen atmosphere; then, 2,2-dimethoxypropane (9.5 mL; 2 equivalents) was added followed by 25 mL of acetone. The reaction was run overnight at room temperature and in inert atmosphere. The reaction progress was controlled by TLC using as eluent a mixture of CH₂Cl₂ and methanol (8:2). In order to remove the acid, 0.290 mL of an ammonia solution were added. Afterward, an extraction in CH₂Cl₂/water was made. The organic phase was dried with anhydrous Na₂SO₄ and, after filtration, the solvent was removed by rotary evaporation.

The compound was collected as a white solid (Yield: 70%). ¹H NMR (400 MHz, Chloroform-*d*) δ 11.14 (s, 1H), 4.18 (d, *J* = 11.9 Hz, 2H), 3.67 (d, *J* = 11.9 Hz, 2H), 1.44 (s, 3H), 1.41 (s, 3H), 1.21 (s, 3H). ¹³C NMR (101 MHz, CDCl₃) δ 180.06, 98.50, 66.03, 41.87, 25.34, 22.13, 18.56.

Compound 2. Compound 1 (252 mg; 1 equivalent), EDC (305 mg; 1.1 equivalents), and DMAP (18 mg; 0.1 equivalents) were put in nitrogen atmosphere. Then, 10 mL of anhydrous CH₂Cl₂ were added and the solution was left in stirring and inert atmosphere for 5 min. Afterward, propargyl alcohol (170 μL; 2 equivalents) was added with a syringe; the reaction was run at room temperature, in stirring and Nitrogen atmosphere overnight. To control the progress of the reaction a TLC was done using as eluent a mixture of hexane and ethyl acetate (8:2). To purify the product, a column chromatography on silica flash was made using the same eluent as those for TLC (rf: 0.42) The product was obtained as an uncoloured oil (Yield: 74%).

¹H NMR (400 MHz, Chloroform-*d*) δ 4.73 (d, *J* = 2.5 Hz, 2H), 4.20 (d, *J* = 11.8 Hz, 2H), 3.65 (d, *J* = 11.8 Hz, 2H), 2.46 (t, *J* = 2.5 Hz, 1H), 1.42 (s, 3H), 1.39 (s, 3H), 1.22 (s, 3H). ¹³C NMR (101 MHz, CDCl₃) δ 172.42, 97.14, 73.93, 67.24, 64.86, 51.33, 40.90, 23.47, 21.75, 17.46.

Compound DG₁. Compound 2 (151 mg; 1 equivalent) was dissolved using 1 mL of Methanol. Separately, sulfuric acid (32μL; 0.85 equivalents) was added to another 1 mL of methanol and then, the solution was added to the previous one followed by another 1 mL of methanol. The reaction was run at room temperature, under stirring for three hours and the progress of the reaction was monitored by TLC using as eluent a mixture of hexane and ethyl acetate (8:2) and the reaction was stopped by adding to the reaction mixture an ammonia

solution (128.5 μL). The salt obtained was removed by filtration on celite and washed with methanol. The compound was obtained as a white solid after rotary evaporation of the solvent (Yield: 99%).

^1H NMR (400 MHz, Methanol- d_4) δ 4.71 (d, J = 2.4 Hz, 2H), 3.75 – 3.59 (m, 4H), 2.89 (t, J = 2.5 Hz, 1H), 1.17 (s, 3H). ^{13}C NMR (101 MHz, MeOD) δ = 175.71, 78.78, 76.18, 65.69, 52.98, 51.59, 17.19.

Compound 3. Compound **1** (566 mg; 5 equivalents), EDC (621 mg; 5 equivalents), and DMAP (40 mg; 0.5 equivalents) were put in nitrogen atmosphere for 5 minutes. Then, 3 mL of anhydrous CH_2Cl_2 were added. Separately, compound **DG**₁ (172 mg; 1 equivalent) was dissolved in other 3 mL of anhydrous CH_2Cl_2 and then, transferred, by means of other 4 mL of solvent, to the reaction mixture. The reaction was run at room temperature, in stirring and Nitrogen atmosphere overnight. To control the progress of the reaction a TLC was done using as eluent a mixture of hexane and ethyl acetate (7:3). To purify the product, a column chromatography on silica flash was made using the same eluent as those for TLC (rf: 0.4) The product was obtained as an uncoloured oil (Yield: 60%).

^1H NMR (400 MHz, Chloroform- d) δ 4.71 (d, J = 2.5 Hz, 2H), 4.32 (s, 4H), 4.14 (d, J = 11.9 Hz, 4H), 3.61 (d, J = 12.0 Hz, 4H), 2.46 (t, J = 2.5 Hz, 1H), 1.40 (s, 6H), 1.35 (s, 6H), 1.31 (s, 3H), 1.15 (s, 6H). ^{13}C NMR (101 MHz, CDCl_3) δ 173.63, 171.96, 98.25, 77.34, 75.43, 66.11, 65.42, 52.81, 46.96, 42.21, 25.07, 22.44, 18.67, 17.72.

Compound DG₂. Compound **3** (170 mg; 1 equivalent) was dissolved using 2 mL of Methanol. Separately, sulfuric acid (32 μL ; 1.7 equivalents) was added to another 1 mL of methanol and then, the acid solution was added to the reaction mixture and other 2 mL of methanol were added. The reaction was run at room temperature, in stirring for three hours and progress of the reaction was monitored by TLC using as eluent a mixture of hexane and ethyl acetate (7:3), and the reaction was stopped by adding to the reaction an ammonia solution (100 μL). The salt obtained was removed by filtration on celite. The compound was obtained as a solid after rotary evaporation of the solvent (Yield: 99%).

^1H NMR (400 MHz, Methanol- d_4) δ 4.76 (d, J = 2.5 Hz, 2H), 4.29 (d, J = 2.7 Hz, 4H), 3.71 – 3.56 (m, 8H), 2.95 (t, J = 2.5 Hz, 1H), 1.31 (s, 3H), 1.15 (s, 6H). ^{13}C NMR (101 MHz, MeOD) δ = 175.88, 173.62, 78.50, 76.65, 66.31, 65.81, 53.55, 51.77, 47.87, 18.05, 17.26.

Compound 4. Compound **1** (517 mg; 8 equivalents), EDC (569 mg; 8 equivalents), and DMAP (23 mg; 0.5 equivalents) were put in nitrogen atmosphere for 5 minutes. Then, 3 mL of anhydrous CH_2Cl_2 were added and the solution was put under three cycles of vacuum/ nitrogen atmosphere. Separately, compound **DG**₂ (150 mg, 1 equivalent) was dissolved in other 5 mL of anhydrous CH_2Cl_2 and then, transferred to the reaction mixture. After the addition of other 5 mL of CH_2Cl_2 , the reaction was run at room temperature, in stirring and nitrogen atmosphere overnight. To control the progress of the reaction a TLC was done using as eluent a mixture of hexane and ethyl acetate (7:3). To purify the product, a column chromatography on silica flash was made using the same eluent as those for TLC (rf: 0.4) The product was obtained as an oil (Yield: 70%). The compound was directly used for the following step.

Compound DG₃. Compound **4** (200 mg; 1 equivalent) was dissolved using 3 mL of Methanol. Separately, sulfuric acid (37 μL ; 3.4 equivalents) was mixed with 1 mL of methanol and then added to the reaction mixture. Other 3 mL of methanol were added; then, the reaction was run at room temperature, in stirring for three hours and progress of the reaction was monitored by TLC using as eluent a mixture of hexane and ethyl acetate (7:3),

and the reaction was stopped by adding to the reaction mixture an ammonia solution (100 μL). The salt was filtered away on celite. The solvent was removed by rotary evaporation and the compound was obtained as a solid (Yield: 99%). ^1H NMR (400 MHz, Methanol- d_4) δ = 4.79 (d, $J=2.5$, 2H), 4.39 – 4.20 (m, 12H), 3.73 – 3.55 (m, 16H), 2.98 (t, $J=2.5$, 1H), 1.32 (s, 3H), 1.30 (s, 6H), 1.15 (s, 12H). ^{13}C NMR (101 MHz, MeOD) δ = 175.92, 173.74, 173.16, 78.53, 76.99, 67.25, 66.20, 65.86, 53.77, 51.79, 47.99, 47.96, 18.24, 17.99, 17.31.

Compound FJD₁. Compound **DG₁** (313 mg; 1 equivalent) and CuI (7 mg; 0.1 equivalents) were dissolved in 500 μL of DMF in inert atmosphere. Separately, **F₂₇-N₃** (62 mg; 1 equivalent) was dissolved in other 500 μL of DMF and transferred to the reaction mixture by means of other 1.5 mL of DMF. The reaction was run in stirring and nitrogen atmosphere at 55 $^\circ\text{C}$ overnight. The formation of the product was confirmed analyzing by FTIR 100 μL aliquot of the solution and monitoring the disappearance of the characteristic stretching of the azido group (2100 cm^{-1}). The reaction was stopped, added to iced water and extracted with CH_2Cl_2 ; then, the organic phase was washed for two times with a 0.1 % disodium EDTA solution and once with a saturated NaCl solution. The organic phase was collected, dried with Na_2SO_4 , and rotary evaporated. The compound was collected as a white solid (Yield: 80%).

^1H NMR (400 MHz, Methanol- d_4) δ 7.96 (s, 1H), 5.23 (s, 2H), 4.46 (t, $J = 7.1$ Hz, 2H), 4.16 (s, 7H), 3.77 – 3.53 (m, 4H), 3.47 (t, $J = 6.1$ Hz, 2H), 3.44 (s, 2H), 2.17 (p, $J = 6.6$ Hz, 2H), 1.15 (s, 3H). ^{13}C NMR (101 MHz, Methanol- d_4) δ 176.23 , 144.36 , 125.72 (d, $J = 50.4$ Hz), 123.28 – 117.10 (m), 81.53 – 80.16 (m), 69.17 , 67.16 , 67.11 , 65.86 , 58.44 , 51.70 , 48.40 , 47.50 , 31.29 , 17.22. ^{13}C NMR (101 MHz, Methanol- d_4) δ 176.23 , 144.36 , 125.47 , 126.28 – 117.17 (q, $^1J_{\text{C-F}} = 291.8$ Hz), 81.83 – 80.16 (m), 69.17 , 67.16 , 67.11 , 65.86 , 58.44 , 51.70 , 48.40 , 47.50 , 31.29 , 17.22. ^{19}F NMR (376 MHz, MeOD) δ -71.51. ATR-FTIR: Stretching O-H: 3650-3000 cm^{-1} ; Stretching C-H: 2970-2800 cm^{-1} ; Stretching C=O: 1726 cm^{-1} ; Stretching C-F: 1300 cm^{-1} ; Bending C-F: 700 cm^{-1} ; HR-MS (ESI) for $\text{C}_{28}\text{H}_{26}\text{F}_{27}\text{N}_3\text{O}_8$ - theoretical $[\text{M-Na}]^+$: 1068.1186/ Found $[\text{M-Na}]^+$: 1068.1166.

Compound FJD₂. Compound **DG₂** (110 mg; 1 equivalent) and CuI (8 mg; 0.15 equivalents) were dissolved in 1 mL of DMF under inert atmosphere. Separately, **F₂₇-N₃** (238 mg; 1 equivalent) was dissolved in other 1.5 mL of DMF and transferred to the reaction mixture. The reaction was run in stirring and nitrogen atmosphere at 55 $^\circ\text{C}$ overnight. The formation of the product was confirmed by analyzing at FTIR 100 μL of the solution by monitoring the disappearance of the characteristic stretching of the azido group (2100 cm^{-1}). The reaction was stopped, added to iced water and extracted with CH_2Cl_2 ; then, the organic phase was washed two times with a 0.1 % disodium EDTA solution and 1 time with a saturated NaCl solution. The organic phase was collected, dried with Na_2SO_4 , and rotary evaporated. The compound was collected as a sticky solid (Yield: 80%).

^1H NMR (400 MHz, Methanol- d_4) δ = 8.08 (s, 1H), 5.31 (s, 2H), 4.53 (t, $J=7.2$, 2H), 4.40 – 4.27 (m, 4H), 4.22 (s, 6H), 3.74 – 3.59 (m, 8H), 3.54 (t, $J=6.1$, 2H), 3.51 (s, 2H), 2.24 (m, 2H), 1.34 (s, 4H), 1.16 (s, 6H). ^{13}C NMR (101 MHz, Methanol- d_4) δ 126.01, 126.72 – 117.13 (q, $^1J_{\text{C-F}} = 292.3$ Hz), 80.97 (m, $^2J_{\text{C-F}} = 30.5$ Hz), 69.21, 67.12, 67.06 , 66.36 , 65.84 , 58.98 , 51.78 , 48.46 , 47.88 , 47.51 , 31.31 , 18.08 , 17.21. ^{19}F NMR (376 MHz, MeOD) δ -71.51.

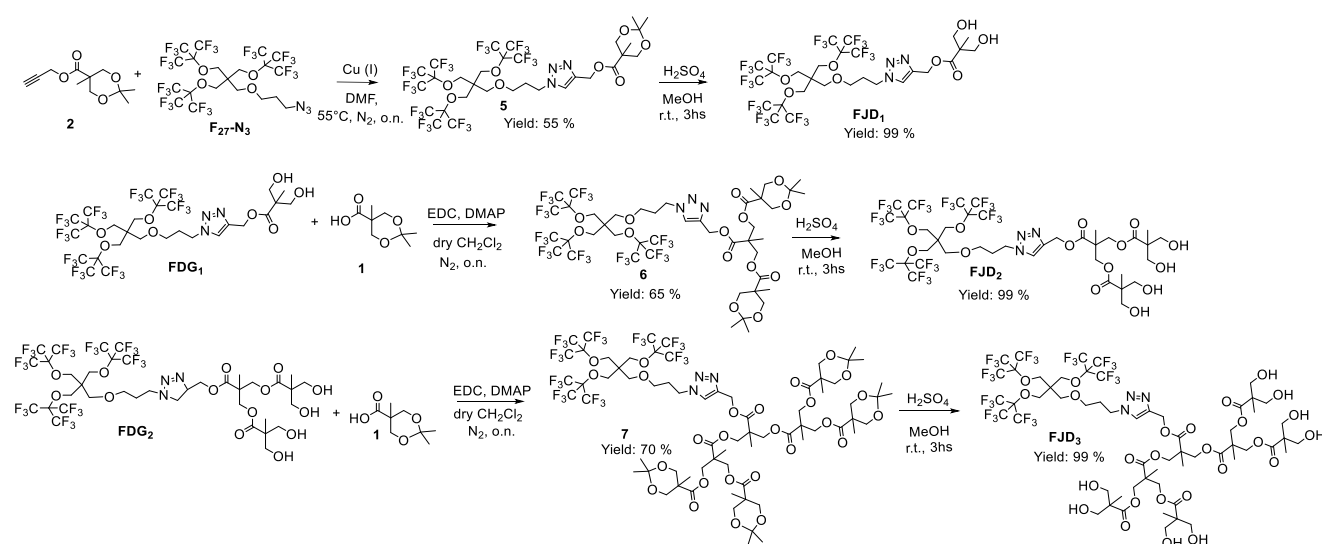
ATR-FTIR: Stretching O-H: 3650-3100 cm^{-1} ; Stretching C-H: 3000-2850 cm^{-1} ; Stretching C=O: 1727 cm^{-1} ; Stretching C-F: 1250 cm^{-1} ; Bending C-F: 700 cm^{-1} ; HR-MS (ESI) for $\text{C}_{38}\text{H}_{42}\text{F}_{27}\text{N}_3\text{O}_{14}$ - theoretical $[\text{M-Na}]^+$: 1300.2133/ Found $[\text{M-Na}]^+$: 1300.2113.

Compound FJD₃. Compound **DG₃** (53 mg; 1 equivalent) and CuI (5.4 mg; 0.5 equivalents) were dissolved in 1 mL of DMF under inert atmosphere. Separately, **F₂₇-N₃** (52 mg; 1 equivalent) was dissolved in other 1.5 mL of DMF and transferred to the reaction mixture. The reaction was run in stirring and nitrogen atmosphere at 55 $^\circ\text{C}$

overnight. The formation of the product was confirmed analyzing FTIR of 100 μL aliquots of the solution and monitoring disappearance of the characteristic stretching of the azido group (2100 cm^{-1}). The reaction was stopped, added to iced water and extracted with CH_2Cl_2 ; then, the organic phase was washed twice with a 0.1 % disodium EDTA solution and once with a saturated NaCl solution. The organic phase was collected, dried with Na_2SO_4 , and rotary evaporated. The compound was collected as a white solid (Yield: 70%).

^1H NMR (400 MHz, Methanol- d_4) $\delta = 8.12$ (s, 1H), 5.34 (s, 2H), 4.55 (t, $J=7.1$, 2H), 4.43 – 4.25 (m, 12H), 4.22 (s, 6H), 3.79 – 3.63 (m, 16H), 3.55 (t, $J=6.1$, 2H), 3.51 (s, 2H), 2.25 (m, 2H), 1.35 (s, 3H), 1.30 (s, 6H), 1.21 (s, 12H). ^{13}C NMR (101 MHz, Methanol- d_4) δ 175.93 , 173.70 , 143.58 , 126.19 , 120.15 (q, $^1J_{\text{C-F}} = 292.5$ Hz), 81.52 – 80.43 (m), 69.24 , 67.24 , 67.11 , 67.06 , 66.16 , 65.87 , 59.09 , 51.81 , 48.49 , 47.97 , 47.93 , 47.51 , 31.33 , 18.17 , 18.00 , 17.30. ^{19}F NMR (376 MHz, MeOD) δ -71.47. ATR-FTIR: Stretching O-H: $3600\text{--}3100\text{ cm}^{-1}$; Stretching C-H: $3000\text{--}2884\text{ cm}^{-1}$; Stretching C=O: 1729 cm^{-1} ; Stretching C-F: 1230 cm^{-1} ; Bending C-F: 700 cm^{-1} ; HR-MS (ESI) for $\text{C}_{58}\text{H}_{74}\text{F}_{27}\text{N}_3\text{O}_{26}$ - theoretical $[\text{M-Na}]^+$: 1764.4027/ Found $[\text{M-Na}]^+$: 1764.4031.

• Synthesis of FJD₁, FJD₂, and FJD₃: Divergent-like approach



Scheme S3: Synthesis of the Janus dendrimers FJD₁₋₃: divergent-like approach.

Compound 5. CuI (12 mg; 0.1 equivalents) was dispersed in 0.5 mL of DMF and then, compound 2 (160 mg; 1 equivalent) was added by means of 1 mL of DMF. Finally, **F₂₇-N₃** (658 mg; 1 equivalent) was added by using other 2 mL of DMF. The reaction was run at 55 °C, in inert atmosphere overnight. The formation of the product was confirmed analyzing FTIR of 100 μL aliquots of the solution and monitoring disappearance of the characteristic stretching of the azido group (2100 cm^{-1}). The reaction was stopped, added to iced water and extracted with CH_2Cl_2 ; then, the organic phase was washed twice with a 0.1 % disodium EDTA solution and once with a saturated NaCl solution. The organic phase was collected, dried with Na_2SO_4 , and rotary evaporated. The compound was collected as oil (Yield: 55%).

^1H NMR (400 MHz, Chloroform- d) δ 7.66 (s, 1H), 5.31 (s, 2H), 4.42 (t, $J = 5.6$ Hz, 2H), 4.20 (d, $J = 11.5$ Hz, 2H), 3.64 (d, $J = 11.4$ Hz, 2H), 3.46 (t, $J = 5.6$ Hz, 2H), 3.40 (s, 2H), 2.18 (m, 2H), 1.42 (s, 3H), 1.34 (s, 3H), 1.15 (s, 3H). ^{19}F NMR (376 MHz, CDCl_3) δ -70.37.

Compound FJD₁. Compound **5** (456 mg; 1 equivalent) was dissolved using 2 mL of Methanol. Separately, sulfuric acid (25 μ L; 1 equivalent) was added to another 1.5 mL of methanol and then, this solution was added to the previous one by means of other 3.5 mL of methanol. The reaction was run at room temperature, in stirring for three hours and progress of the reaction was monitored by TLC using as eluent a mixture of hexane and ethyl acetate (7:3), and the reaction was stopped adding to the reaction mixture an ammonia solution (267 μ L). The salt obtained was removed by filtration on celite and washed with methanol which was, then, removed by rotary evaporation. The compound was obtained as a solid (Yield: 99%).

¹H NMR (400 MHz, Methanol-*d*₄) δ 7.96 (s, 1H), 5.23 (s, 2H), 4.46 (t, *J* = 7.1 Hz, 2H), 4.16 (s, 7H), 3.77 – 3.53 (m, 4H), 3.47 (t, *J* = 6.1 Hz, 2H), 3.44 (s, 2H), 2.17 (p, *J* = 6.6 Hz, 2H), 1.15 (s, 3H). ¹³C NMR (101 MHz, Methanol-*d*₄) δ 176.23 , 144.36 , 125.72 (d, *J* = 50.4 Hz), 123.28 – 117.10 (m), 81.53 – 80.16 (m), 69.17 , 67.16 , 67.11 , 65.86 , 58.44 , 51.70 , 48.40 , 47.50 , 31.29 , 17.22. ¹³C NMR (101 MHz, Methanol-*d*₄) δ 176.23 , 144.36 , 125.47 , 126.28 – 117.17 (q, ¹*J*_{C-F} = 291.8 Hz), 81.83 – 80.16 (m), 69.17 , 67.16 , 67.11 , 65.86 , 58.44 , 51.70 , 48.40 , 47.50 , 31.29 , 17.22. ¹⁹F NMR (376 MHz, MeOD) δ -71.51. ATR-FTIR: Stretching O-H: 3650-3000 cm⁻¹; Stretching C-H: 2970-2800 cm⁻¹; Stretching C=O: 1726 cm⁻¹; Stretching C-F: 1300 cm⁻¹; Bending C-F: 700 cm⁻¹; HR-MS (ESI) for C₂₈H₂₆F₂₇N₃O₈ - theoretical [M-Na]⁺: 1068.1186/ Found [M-Na]⁺: 1068.1166.

Compound 6. Compound **1** (522 mg; 6 equivalents), EDC (574 mg; 6 equivalents), and DMAP (31 mg; 0.5 equivalents) were put in nitrogen atmosphere for 5 minutes. Then, 3 mL of anhydrous CH₂Cl₂ were added and the solution was treated with three cycles of vacuum/ nitrogen. Separately, compound **FJD₁** (522 mg, 1 equivalent) was dissolved in other 5 mL of anhydrous CH₂Cl₂ and then, transferred, by means of other 7 mL of the solvent, to the reaction mixture. The reaction was run at room temperature, in stirring and nitrogen atmosphere overnight. To control progress of the reaction a TLC was done using as eluent a mixture of hexane and ethyl acetate (7:3). To purify the product, a column chromatography on silica flash was made using the same eluent as those for TLC (rf: 0.5) The product was obtained as a pale-yellow oil (Yield: 65%). The compound was directly used for the following step.

Compound FJD₂. Compound **6** (300 mg; 1 equivalent) was dissolved in 2 mL of Methanol. Separately, sulfuric acid (24 μ L; 1.7 equivalent) was dissolved in 1mL of methanol and added to the reaction mixture. After the addition of further 3 mL of methanol, the reaction was run at room temperature, in stirring for three hours and progress of the reaction was monitored by TLC using as eluent a mixture of hexane and ethyl acetate (7:3). The reaction was stopped adding to the reaction mixture an ammonia solution (250 μ L). The salt obtained was removed by filtration on celite and washed with methanol which was, then, removed by rotary evaporation. The compound was obtained as a solid (Yield: 99%).

¹H NMR (400 MHz, Methanol-*d*₄) δ = 8.08 (s, 1H), 5.31 (s, 2H), 4.53 (t, *J*=7.2, 2H), 4.40 – 4.27 (m, 4H), 4.22 (s, 6H), 3.74 – 3.59 (m, 8H), 3.54 (t, *J*=6.1, 2H), 3.51 (s, 2H), 2.24 (m, 2H), 1.34 (s, 4H), 1.16 (s, 6H). ¹³C NMR (101 MHz, Methanol-*d*₄) δ 126.01 , 126.72 – 117.13 (q, ¹*J*_{C-F} = 292.3 Hz), 80.97 (m, ²*J*_{C-F} = 30.5 Hz), 69.21 , 67.12 , 67.06 , 66.36 , 65.84 , 58.98 , 51.78 , 48.46 , 47.88 , 47.51 , 31.31 , 18.08 , 17.21. ¹⁹F NMR (376 MHz, MeOD) δ -71.51. ATR-FTIR: Stretching O-H: 3650-3100 cm⁻¹; Stretching C-H: 3000-2850 cm⁻¹; Stretching C=O: 1727 cm⁻¹; Stretching C-F: 1250 cm⁻¹; Bending C-F: 700 cm⁻¹; HR-MS (ESI) for C₃₈H₄₂F₂₇N₃O₁₄- theoretical [M-Na]⁺: 1300.2133/ Found [M-Na]⁺: 1300.2113.

Compound 7. Compound **1** (246 mg; 12 equivalents), EDC (271 mg; 12 equivalents), and DMAP (17 mg; 1.1 equivalents) were put in nitrogen atmosphere for 5 minutes. Then, 2 mL of anhydrous CH₂Cl₂ were added and the solution was treated with three cycles of vacuum/ nitrogen atmosphere. Separately, compound **FJD**₂ was dissolved in other 3 mL of anhydrous CH₂Cl₂ to the reaction mixture. The reaction was run at room temperature, in stirring and Nitrogen atmosphere overnight. To control the progress of the reaction a TLC was done using as eluent a mixture of hexane and ethyl acetate (4:6). To purify the product, a column chromatography on silica flash was made using the same eluent as those for TLC (rf: 0.7) The product was obtained as an oil (Yield: 70%). The compound was directly used for the following step.

Compound FJD₃. Compound **7** (162 mg; 1 equivalent) was dissolved using 1.5 mL of Methanol. Separately, sulfuric acid (25 μ L; 7.7 equivalent) was added to another 0.5 mL of methanol and then, this solution was added to the previous one by means of other 1 mL of methanol. The reaction was run at room temperature, in stirring for three hours and progress of the reaction was monitored by TLC using as eluent a mixture of hexane and ethyl acetate (4:6), and the reaction was stopped by adding to the reaction mixture an ammonia solution (267 μ L). The salt obtained was removed by filtration on celite and washed with methanol which was, then, removed by rotary evaporation. The compound was obtained as a solid (Yield: 99%).

¹H NMR (400 MHz, Methanol-*d*₄) δ = 8.12 (s, 1H), 5.34 (s, 2H), 4.55 (t, *J*=7.1, 2H), 4.43 – 4.25 (m, 12H), 4.22 (s, 6H), 3.79 – 3.63 (m, 16H), 3.55 (t, *J*=6.1, 2H), 3.51 (s, 2H), 2.25 (m, 2H), 1.35 (s, 3H), 1.30 (s, 6H), 1.21 (s, 12H). ¹³C NMR (101 MHz, Methanol-*d*₄) δ 175.93 , 173.70 , 143.58 , 126.19 , 120.15 (q, ¹*J*_{C-F} = 292.5 Hz), 81.52 – 80.43 (m), 69.24 , 67.24 , 67.11 , 67.06 , 66.16 , 65.87 , 59.09 , 51.81 , 48.49 , 47.97 , 47.93 , 47.51 , 31.33 , 18.17 , 18.00 , 17.30. ¹⁹F NMR (376 MHz, MeOD) δ -71.47. ATR-FTIR: Stretching O-H: 3600-3100 cm⁻¹; Stretching C-H: 3000-2884 cm⁻¹; Stretching C=O: 1729 cm⁻¹; Stretching C-F: 1230 cm⁻¹; Bending C-F: 700 cm⁻¹; HRMS (ESI) for C₅₈H₇₄F₂₇N₃O₂₆ - theoretical [M-Na]⁺: 1764.4027/ Found [M-Na]⁺: 1764.4031.

- **Single Crystal X-ray diffraction analysis - Structural characterization of FJD**₁

Data collections were performed at the X-ray diffraction beamline (XRD1) of the Elettra Synchrotron, Trieste (Italy).^[S3] The crystals were dipped in NHV oil (Jena Bioscience, Jena, Germany) and mounted on the goniometer head with kapton loops (MiTeGen, Ithaca, USA). Complete datasets were collected at 100 K (nitrogen stream supplied through an Oxford Cryostream 700) through the rotating crystal method. Data were acquired using a monochromatic wavelength of 0.700 Å on a Pilatus 2M hybrid-pixel area detector (DECTRIS Ltd., Baden-Daettwil, Switzerland). The diffraction data were indexed and integrated using XDS.^[S4] Scaling have been done using CCP4-Aimless code, merging two different datasets from two different crystals to minimize radiation damage effects.^[S5, S6]

The structures were solved by the dual space algorithm implemented in the SHELXT code.^[S7] Fourier analysis and refinement were performed by the full-matrix least-squares methods based on F² implemented in SHELXL (version 2018/3).^[S8] The Coot program was used for modelling.^[S9] **FJD**₁ molecules are tightly packed in a centrosymmetric triclinic unit cell and no solvent molecules have been found in the crystals. **FJD**₁ molecules form dimers (related by crystallographic inversion centers) linked by hydrogen bonds, involving hydroxyl groups and triazole rings of neighbour molecules. Dimers are stacked along the crystallographic *b* axis, through contacts among closest -OH groups. π ·· π stacking interactions among triazole of neighbour dimers can be also found.

Pictures were prepared using CCDC Mercury software.^[S10] Table S.1 shows the crystallographic data for **FJD**₁.

Table S.1 Crystallographic data for FJD₁

FJD₁	
CCDC Number	2009095
Chemical Formula	C ₂₈ H ₂₆ F ₂₇ N ₃ O ₈
Formula weight	1045.52 g/mol
Temperature	100(2) K
Wavelength	0.700 Å
Crystal system	Triclinic
Space Group	<i>P</i> -1
Unit cell dimensions	<i>a</i> = 10.408(2) Å <i>b</i> = 10.676(2) Å <i>c</i> = 20.331(4) Å <i>α</i> = 80.69(3)° <i>β</i> = 88.28(3)° <i>γ</i> = 62.80(3)°
Volume	1980.4(9) Å ³
Z	2
Density (calculated)	1.753 g·cm ⁻³
Absorption coefficient	0.196 mm ⁻¹
F(000)	1044
Crystal size	0.10·0.05·0.02 mm ³
Crystal habit	Transparent thin needles
Theta range for data collection	1.0° to 31.2°
Index ranges	-14 ≤ <i>h</i> ≤ 14, -15 ≤ <i>k</i> ≤ 15, -29 ≤ <i>l</i> ≤ 29
Reflections collected	46019
Independent reflections	11910, 8468 data with <i>I</i> > 2σ(<i>I</i>)
Data multiplicity (max resltn)	3.81 (3.32)
<i>I</i> /σ(<i>I</i>) (max resltn)	3.74 (2.34)
Rmerge (max resltn)	0.1023 (0.3216)
Data completeness (max resltn)	98.7% (96.7%)
Refinement method	Full-matrix least-squares on F ²
Data / restraints / parameters	8468 / 120 / 709
Goodness-of-fit on F ²	1.030
Δ/σmax	0.005
Final R indices [<i>I</i> > 2σ(<i>I</i>)]	R ₁ = 0.0834, wR ₂ = 0.2441
R indices (all data)	R ₁ = 0.1080, wR ₂ = 0.2776
Largest diff. peak and hole	0.757 and -0.717 eÅ ⁻³
R.M.S. deviation from mean	0.078 eÅ ⁻³

$$R_1 = \frac{\sum ||F_o| - |F_c||}{\sum |F_o|}, wR_2 = \left\{ \frac{\sum [w(F_o^2 - F_c^2)^2]}{\sum [w(F_o^2)^2]} \right\}^{1/2}$$

Powder X-ray diffraction analysis - Structural characterization of FJD₁

Powder X-Ray diffraction data of compound **FJD₁** were collected on Bruker AXS D8 powder diffractometer with experimental parameters as follows: Cu-K α radiation ($\lambda = 1.54056 \text{ \AA}$), scanning interval 4-40° at 2 θ , step size 0.016°, exposure time 1.5 s per step.

- **Thermal analysis and SWAXS characterization**

Thermogravimetric analysis

TGA was done with a Q500 instrument. 1-5 mg of the sample were placed in the melting pot and submitted to a ramp of temperature from 30 °C to 550 °C

Polarized Optimal Microscope

The LC textures and phase transitions were studied with an Olympus BX51 polarized optical microscope equipped with a Linkam Scientific LTS 350 heating stage and a Sony CCD-IRIS/RGB video camera.

Differential Scanning Calorimetry

The enthalpies were measured by differential scanning calorimetry (DSC) with a Mettler Toledo DSC823e operated at a scanning rate of 5°C min⁻¹ on heating and on cooling. Mettler STARe software was used for calculation. An exact amount of the solids (1-5 mg) was weighted and put on aluminium light 20 μ L sample pans.

Small and wide-angle X-Ray spectroscopy

The SWAXS patterns were obtained with a transmission Guinier-like geometry. A linear focalized monochromatic Cu K α 1 beam ($\lambda = 1.5405 \text{ \AA}$) was obtained using a sealed-tube generator (600 W) equipped with a bent quartz monochromator. The samples were filled in home-made sealed cells of 1 mm path. The sample temperature was controlled within $\pm 0.01 \text{ }^\circ\text{C}$, and exposure times were varied from 4 to 24 h. The patterns were recorded with a curved Inel CPS120 counter gas-filled detector (periodicities up to 90 \AA) and on image plates scanned by Amersham Typhoon IP with 25 μ m resolution (periodicities up to 120 \AA). I(2q) profiles were obtained from images, by using home-developed software.

- **Self-assembly in solution**

The ethanol in water procedure

The solid was dissolved in ethanol, then was flash injected with a syringe to MilliQ water. The dispersion was mixed at vertex for 20 seconds at 8 rpm. The dispersions were analyzed overtime.

Table S.2 The ethanol in water procedure. Composition of the analyzed dispersions.

Compound	Weight (mg) (± 0.01)	Volume of Ethanol	Concentration in Ethanol	Water volume	Final Concentration
FJD ₁	1.1	100 μ L (5% v/v)	10 mg/mL	2 mL	0.5 mM
FJD ₂	1.0	100 μ L (5% v/v)	10 mg/mL	2 mL	0.4 mM
FJD ₃	1.1	100 μ L (5% v/v)	10 mg/mL	2 mL	0.3 mM
FJD ₁	0.7	100 μ L (5% v/v)	6.6 mg/mL	2 mL	0.3 mM
FJD ₂	0.8	100 μ L (5% v/v)	8 mg/mL	2mL	0.3 mM

Dynamic light scattering

Data analysis was performed according to standard procedures and the Laplace inversion of the time autocorrelation functions was obtained through a non-cumulant method using CONTIN algorithm, suitable for multimodal and polydisperse systems. Multiangle DLS was measured at ALV compact goniometer system, equipped with ALV-5000/EPP Correlator, special optical fiber detector and ALV/GCS-3 Compact goniometer, with He-Ne laser (= 633 nm, 22 mW output power) as light source. The temperature was controlled with a thermostatic bath and set at 25 °C. A volume comprised between 800 μ l and 1 ml was used for the analysis. DLS was measured at different time points (0, 24, 48 h) and scattering angles $\theta = 70 - 130^\circ$ in 20° steps. Each measure was the result of an average of three subsequent runs of 10 seconds each. Data analysis was done with ALV-Correlator software.

¹⁹F-NMR analysis

400 μ l of the sample were added to 40 μ L of deuterated water (D₂O) and 256 scansions were acquired; NMR spectra for the characterization of the self-assembled nanostructures were measured at different time points (0, 24, 48 h and 6 days).

Cryogenic Transmission Electron Microscopy Imaging:

The cryogenic transmission electron microscopy (Cryo-TEM) images were collected using a JEM 3200FSC field emission microscope (JEOL) operated at 300 kV in bright field mode with Omega-type Zero-loss energy filter. For specimen preparation, 200 mesh copper grids with lacey carbon support film (Electron Microscopy Sciences) were used. Prior to specimen preparation, the TEM grids were plasma cleaned using Gatan Solarus (Model 950) plasma cleaner for 30 seconds. The specimen were prepared by placing 3.0 μ L of a aqueous dispersion of the sample on plasma treated TEM grids and plunge-freezed into -170 °C ethane/propane mixture using Leica automatic plunge freezer EM GP2 with 2 s blotting time. The the relative humidity of 100% was maintained during preparation process. The vitrified specimen was cryo-transferred to the microscope. The images were acquired with Gatan Digital Micrograph® software while the specimen temperature was maintained at -187 °C.

Transmission Electron Microscopy

Transmission electron microscopy (TEM) images were acquired by using a DeLong America LVEM5, equipped with a field emission gun and operating at 5 kV. Samples were prepared by placing 10 μL of the solution on 200 mesh carbon-coated copper grids, leaving the drop on the grid surface for 1 min and finally removing the excess of solvent and dry at air.

- **AA-MD simulations details**

All Atoms MD simulations were run by means of AMBER16 simulation package [Case, D. A.; Betz, R.M.; Cerutti, D.S.; Cheatham, T.E., III; Darden, T.A.; Duke, R.E.; Giese, T.J.; Gohlke, H.; Goetz, A.W.; Homeyer, N.; et al. AMBER16; University of California: San Francisco, CA, USA, 2016], with a simulation length of 100 ns, adopting the general AMBER force field parameters (GAFF) for dendrimers and co-solvent, TIP3P model for water. AM1-BCC charges were used for ethanol, trifluoroethanol and FJD₃.

The simulation on FJD₃ monomer has been run on a truncated octahedral box of 59 Å length, containing 54/4381 and 313/3479 ethanol/water molecules ratios for the 5% and 25% ethanol concentration, respectively, and 51/4341 TFE/water molecules ratios for the 5% of TFE concentration.

For the simulations of dimer, we used a larger truncated octahedral box of 103 Å length, containing 386/24490 and 1951/20066 ethanol/water molecules ratio for the 5% and 25% ethanol concentration, respectively, and 320/26545 TFE/water molecules ratios for the 5% of TFE concentration. The initial configuration of the dimer simulation boxes has been generated by separating the two monomers at an interatomic distance larger than two times the simulation cutoff (10 Å), with each dendrimer fully solvated, in order to prevent the introduction of an external bias. After the initial equilibration phase, in all the three simulations, the two monomers approach each other by diffusion, and then engage mainly via intermolecular non-covalent F-F interactions between the two perfecta moieties. Perfecta branches of the two FJD₃ remains then interlocked over all the rest of the simulation time. For all simulations, systems were initially minimized for 35000 steps and then heated at the target temperature of 300 K over 250000 steps. The minimized structures have been then annealed using the following procedure: from 300K to 1000K for 10⁵ steps ($\Delta T = 100\text{K}$) and then from 1000K to 300K for other 10⁵ steps ($\Delta T = 100\text{K}$). Then, a 2 ns NPT equilibration procedure has been applied, followed by a 100 ns of NPT production dynamics, with SHAKE constraints on solute and co-solvent molecules, using the Langevin dynamics as thermostat and the Berendsen barostat.

- **AA-MD dimer simulations conformational analysis**

Figure S17 displays the Radial Density Functions (RDF) in the monomer simulations calculated between the major atom types of dendrimer and co-solvent with different solvent composition in the box. RDF, normalized by means of the average particle density of the selected atom group, have been calculated using the AMBER16 RDF tool in the three different solvation conditions between i) the dendrimer perfecta-fluorine atoms and the terminal hydrogen atoms of the CH₃ ethanol group (fluorine atoms of the CF₃ TFE group), ii) the dendrimer sp³ carbon atoms with the ethanol (TFE) sp³ carbon atoms; iii) the nitrogen atoms of dendrimer triazole moiety with the ethanol (TFE) sp³ carbons and d) the dendrimer carbonyl oxygens with hydrogen termination of the ethanol (TFE) OH group. Figure S17 aids in the identification of different types of favourable solvation interactions between the two co-solvents and the dendrimer atomic groups. In particular, we can see how the ethanol preferentially interacts with FJD₃ hydrophilic chains via hydrogen bonds, while TFE shows a double strong interaction with dendrimer, both via F-F and hydrogen non-covalent bonds, with perfecta moiety and polyester

chains, respectively, highlighting its amphiphilic and highly polar character. Importantly, none of the two co-solvents seems favourably interacting with the central triazole moiety of FJD₃ (see Figure S17c).

Figure S18 shows a representative snapshot of the AA-MD dynamics of the dimer where the hydrophilic, fluorinated and core moieties are surrounded by spheres. It was apparent that the system can be divided in 8 regions of similar sizes. On average, the behavior of the central dihedral angle of the two molecules was similar to that observed for the single molecule, figure S18b. Figure S18c shows that in the presence of 5% of co-solvent, be it ethanol or TFE, R_g was similar that was the FJD₃ molecules have a similar effective size. Figure S18d shows that water was the most efficient medium to bring together the fluorinated moieties of the two dendrimer molecules. The remaining RDF's, figures Figures S18 e-f, show that TFE was structured around the fluorinated end of FJD₃ and the associate presence of short contacts between the carbonyls of FJD₃ and the fluorine atoms of TFE. Figure S19 shows two representative snapshots of trans-oid and cis-oid dimer conformations.

- **Coarse-grain simulations details**

All CG MD simulations were run with LAMMPS package [Thompson, A.P.; Aktulga, H. M.; Berger, R.; Bolintineanu, D. S.; Brown, W. M.; Crozier, P. S.; in 't Veld, P. J.; Kohlmeyer, A.; Moore, S. G.; Nguyen, T. D.; Shan, R.; Stevens, M. J.; Tranchida, J.; Trott, C.; Plimpton, S. J. LAMMPS - a flexible simulation tool for particle-based materials modeling at the atomic, meso, and continuum scales. *Comp Phys Comm.* 2022, 27, 10817]. The parameters used in the Dissipative Particle Dynamics (DPD) associated to the implemented CG model described in the main text are given in Table S3. Each calculation was run in the (N, V, T) ensemble for 5000000 steps for the smaller box of dimensions 40rc x 40rc x 40rc, and for 2500000 steps in the larger box of dimensions 80rc x 80rc x 80rc, with a time step of $\Delta t=0.02\tau$, where τ was the DPD unit of time deriving from the choice of using the mass of particles, the interaction range and the temperature as unit of mass, length and energy (i.e, $m = kT = rc = 1$; $\tau = 1 = \sqrt{m/kT}$); A time-reversible Verlet with the rESPA integrator derived by Tuckerman et al. [Tuckerman, M.; Berne, B.J. Reversible multiple time scale molecular dynamics. *J. Chem. Phys.* 1992, 97, 1990] was used in combination with the Nosè-Hoover thermostat [Nosé, S. A unified formulation of the constant temperature molecular dynamics methods. *J. Chem. Phys.* 1984, 81 (1), 511–519]. The dissipative parameter γ was set to 4.5 and the noise amplitude σ to 3; Two additional bonding forces were introduced: a harmonic spring to model the bonding between dendrimer beads, $E = K_r(r - r_0)^2$, and an angle spring interaction, $= K_\theta(\theta - \theta_0)^2$, to properly reproduce the flexibility of the structure. Table S4 reports all the spring and bending constants, K_r and K_θ , respectively, with the equilibrium distances and angles, r_0 , and θ_0 , adopted in this work.

The initial simulation boxes were prepared via Moltemplate Molecular Building for LAMMPS [Jewett, A.I.; Stelter, D.; Lambert, J.; Saladi, S. M.; Roscioni, O.M.; Ricci, M.; Autin, L.; Maritan, M.; Bashusqeh, S. M.; Keyes, T.; Dame, R.T.; Shea, J.-E.; Jensen, G.J.; Goodsell, D.S. Moltemplate: A Tool for Coarse-Grained Modeling of Complex Biological Matter and Soft Condensed Matter Physics. *J. Mol. Biol.* 2021, 433(11),166841] and then equilibrated for 175000. In order to ensure a highly degree of solvation, we used two extreme interaction parameters during the equilibration procedure, i.e., $a_{ij}=80$ for all dendrimer-dendrimer interactions and $a_{ij}=25$ for every dendrimer group and water.

Table S3. Bead pairs interaction parameters.^a

	a_{ij}					
	CF	OA	OC	S	EC/TC	EO/TO
CF	25	75	75	75	75/10	75/75
OA	75	25	50	30	75/75	20/20
OC	75	50	25	75	50/75	75/75
S	75	30	75	25	75/75	25/25
EC/TC	75/10	75/75	50,75	75/75	25/25	75/75
EO/TO	75/75	20/20	75/75	25/25	75/75	25/25

^a The conservative force parameters a_{ij} are in $k_B T/r_c$ units. Labels of dendrimer beads are described in the text and represented in Figure S20. “S” refers to a water bead.

Table S4. Bond and bond angle parameters

Bead Pair	kr	r0
CF OC	100	0.86
OC OC	100	0.86
OC OA	100	0.86
Bead triples	Kθ	θ
CF OC CF	128	109.5
CF OC OC	128	109.5
OC OC OC	20	180
OC OC OA	20	180
OA OC OA	20	180

- **Snapshots of morphologies of aggregates forming in pure water with 40rc x 40rc x 40rc simulation box**

Figure S20 reports the comparison between the FJD₃ molecular structure and the bead mapping of the coarse grain model. The three different morphologies observed during the CG simulations in water are reported for different a_{OAS} parameters, namely $a_{OAS} = 20, 30$ and 35 , in $40r_c \times 40r_c \times 40r_c$ simulation box in Figure S21. With the strongest hydrophilicity, ($a_{OAS} = 20$), uni-lamellar vesicles with a cavity diameter of about 10 nm and a double layer thickness of 6 nm were obtained, together with disk-like structures. At $a_{OAS} = 30$, uni-lamellar larger irregular vesicles were formed, resulting from the fusion of nearby vesicles, characterized by a smaller inner cavity of 9 nm. At the lowest hydrophilic parameter, $a_{OAS} = 35$, the inner cavity closes and the formation of tubular micelles can be observed.

Figure S22 is the plot of the mean aggregation number calculated from the trajectory of the CG simulation conducted in pure water with $a_{OAS} = 30$ and a box dimension of $80r_c \times 80r_c \times 80r_c$, while Figure S23 describes the corresponding formation of multilamellar vesicles, showing a series of snapshots taken at simulation times where the mean aggregation number drastically increases (corresponding to vertical bars of Figure S22).

The mean aggregation number (N_{agg}) in time, reported in Figure S22, has been calculated as

$$N_{agg} = \frac{\sum_{N > N_{CUT}} N^2 P(N)}{\sum_{N > N_{CUT}} N P(N)} \quad (1)$$

where N is the number of dendrimers, N_{CUT} , set to 125, is the smallest number of dendrimers that forms a distinct cluster, $P(N)$ is the cluster probability distribution calculated at each time step. The distance within which beads of nearby dendrimers were considered to belong to the same cluster was set to 1 nm.

- **Figures**

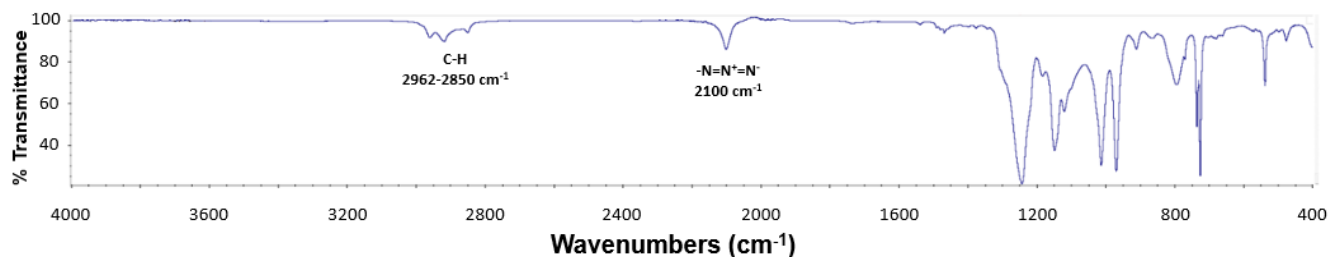


Figure S1 ATR-FTIR spectrum of $F_{27}-N_3$. The presence of the characteristic stretching of the azido group, at 2100cm^{-1} , and the presence of characteristic stretching and bending of C-F between 1300 and 700 cm^{-1} confirmed the structure.

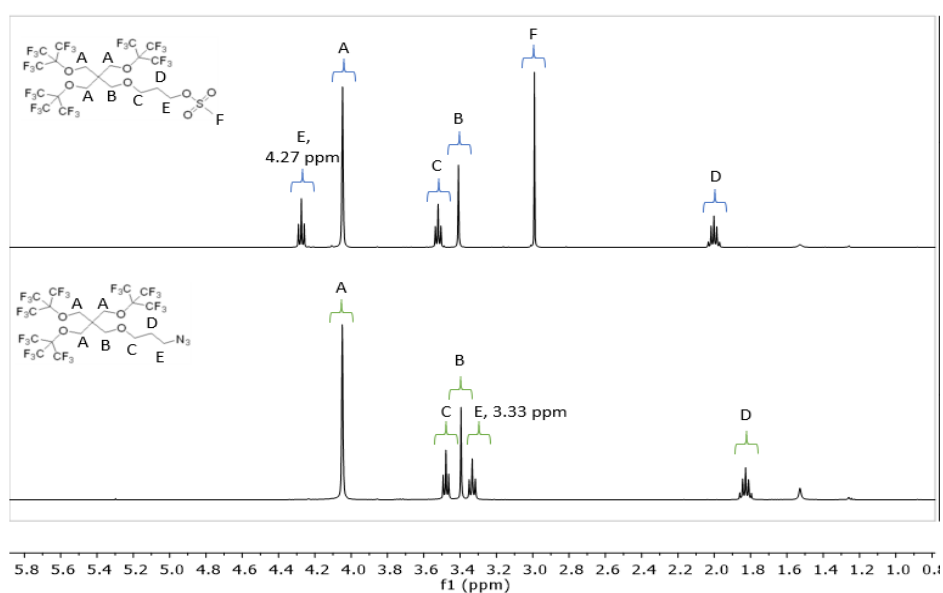


Figure S2 Comparison between the ^1H -NMR spectrum of the $F_{27}-N_3$ derivative and its mesyl precursor (compound d). Solvent CDCl_3 .

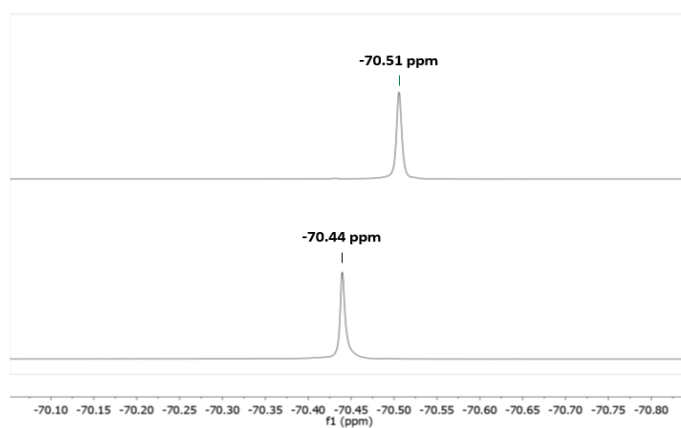


Figure S3 Comparison between the ^{19}F -NMR spectrum of $F_{27}-N_3$ (down) and compound d (up). Solvent: CDCl_3 .

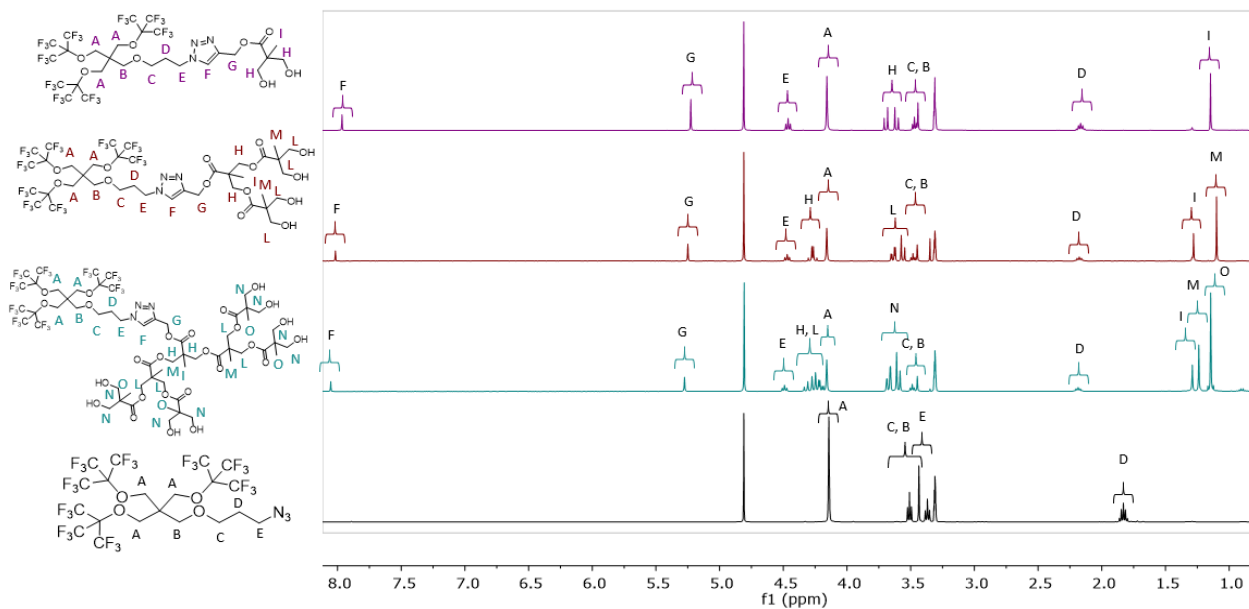


Figure S4 Comparison between ^1H -NMR spectra of FJD₁ (violet), FJD₂ (red), and FJD₃ (light blue) and their fluorinated precursor (F₂₇-N₃, black). Solvent: CD₃OD.

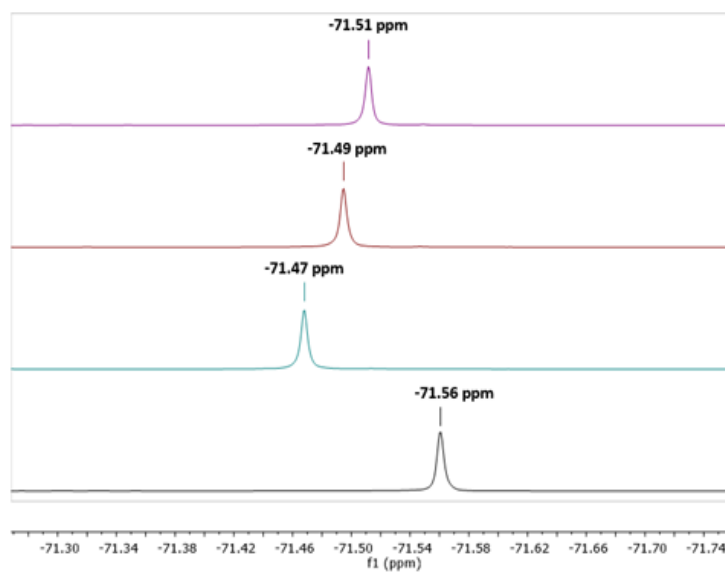


Figure S5 Comparison between ^{19}F -NMR spectra of FJD₁, FJD₂, and FJD₃ and their fluorinated precursor (F₂₇-N₃). Solvent: CD₃OD. Colour code: F₂₇-N₃: black, FJD₁: violet, FJD₂: red, FJD₃: light blue.

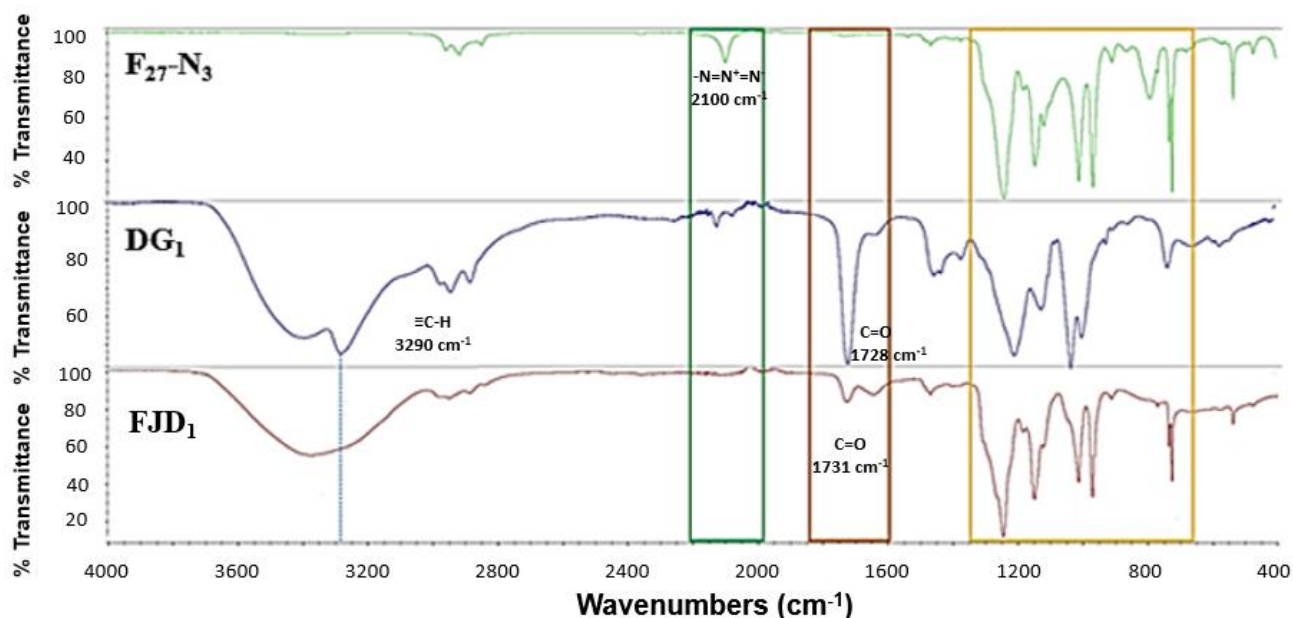


Figure S6 ATR-FTIR spectra comparison between FJD₁, DG₁ alkyne terminating precursor, and F₂₇-N₃. Disappearance of the characteristic stretching of the N=N=N group of F₂₇-N₃ a 2100 cm⁻¹, highlighted in the green rectangle, and disappearance of the ≡C-H stretching of DG₁ precursor at 3300 cm⁻¹, blue dotted line, confirmed the linkage between two molecules. Furthermore, the presence of C=O stretching at 1731 cm⁻¹ and characteristic stretching and bending vibrations of the C-F groups in the range between 1300 cm⁻¹ and 700 cm⁻¹ confirmed the structure of FJD₁.

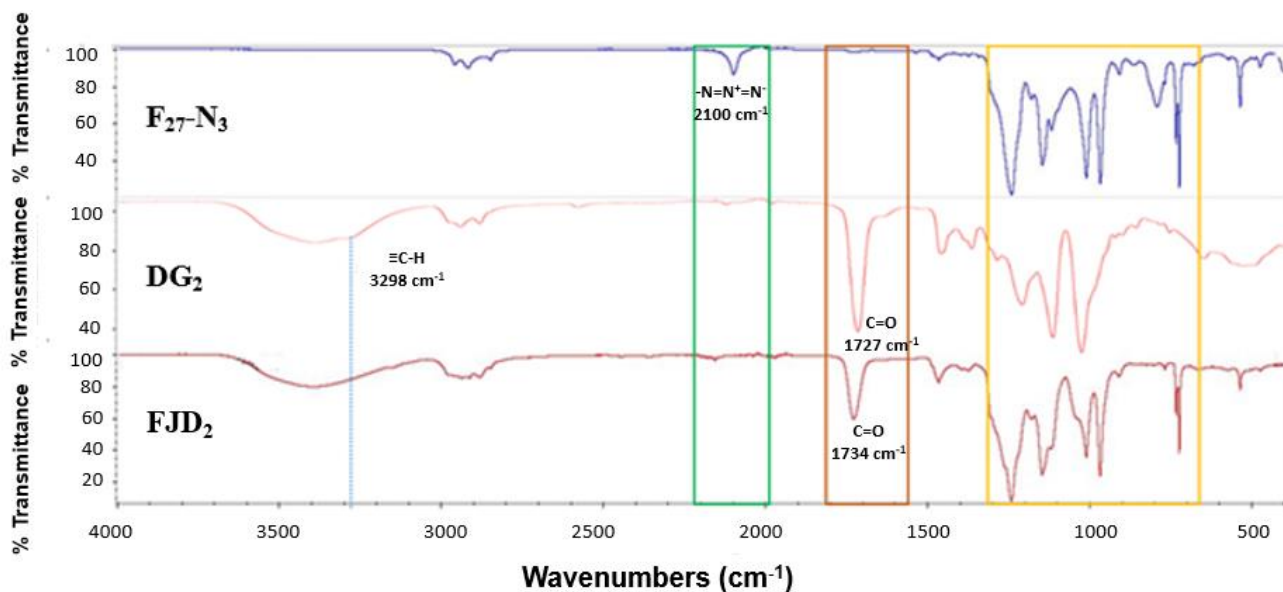


Figure S7 ATR-FTIR spectra comparison between FJD₂, DG₂ alkyne terminating precursor, and F₂₇-N₃. The disappearance of the characteristic stretching of the N=N=N group of F₂₇-N₃ a 2100 cm⁻¹, highlighted in the green rectangle, and disappearance of the ≡C-H stretching of DG₂ precursor at 3298 cm⁻¹, blue dotted line, confirmed the linkage between two molecules. Furthermore, the presence of C=O stretching at around 1730 cm⁻¹ and characteristic stretching and bending vibrations of C-F groups in the range between 1300 cm⁻¹ and 700 cm⁻¹ confirmed the structure of FJD₂.

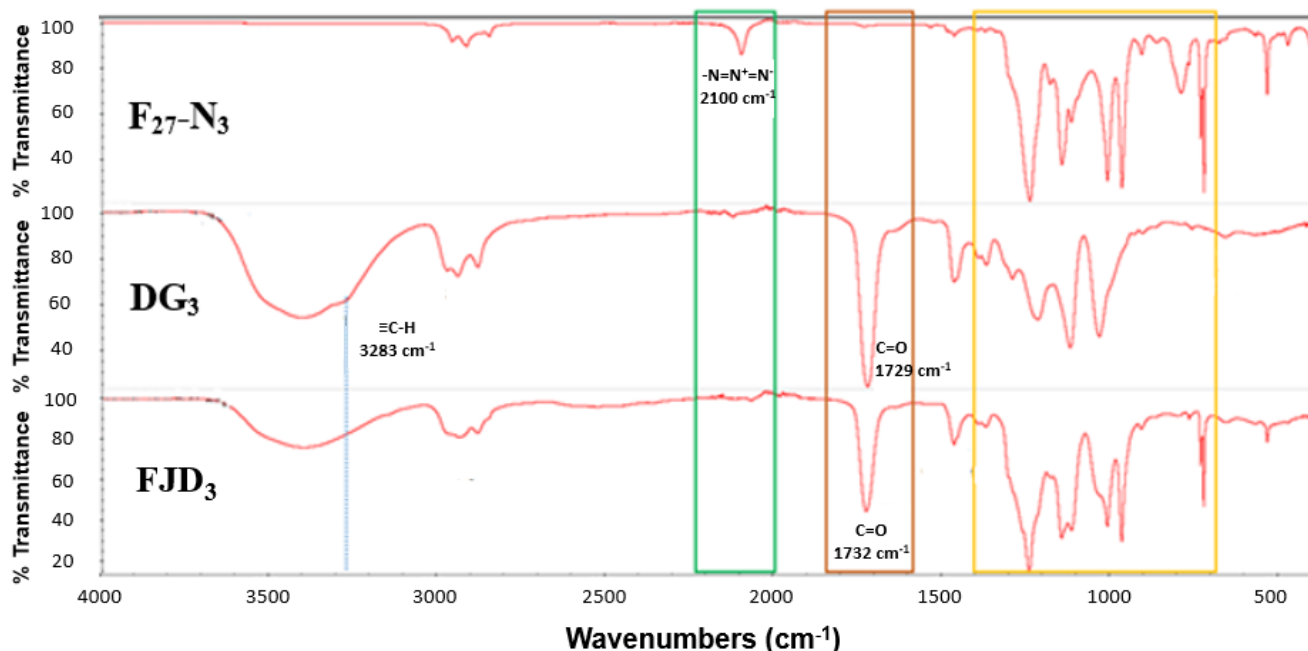


Figure S8 ATR-FTIR spectra comparison between FJD₃, DG₃ alkyne terminating precursor, and F₂₇-N₃. The disappearance of the characteristic stretching of the N=N=N group of F₂₇-N₃ at 2100 cm⁻¹, highlighted in the green rectangle, and disappearance of the ≡C-H stretching of DG₃ precursor at 3283 cm⁻¹, blue dotted line, confirmed the linkage between two molecules. Furthermore, the presence of C=O stretching at around 1730 cm⁻¹ and of characteristic stretching and bending vibrations of C-F groups in the range between 1300 cm⁻¹ and 700 cm⁻¹ confirmed the structure of FJD₃.

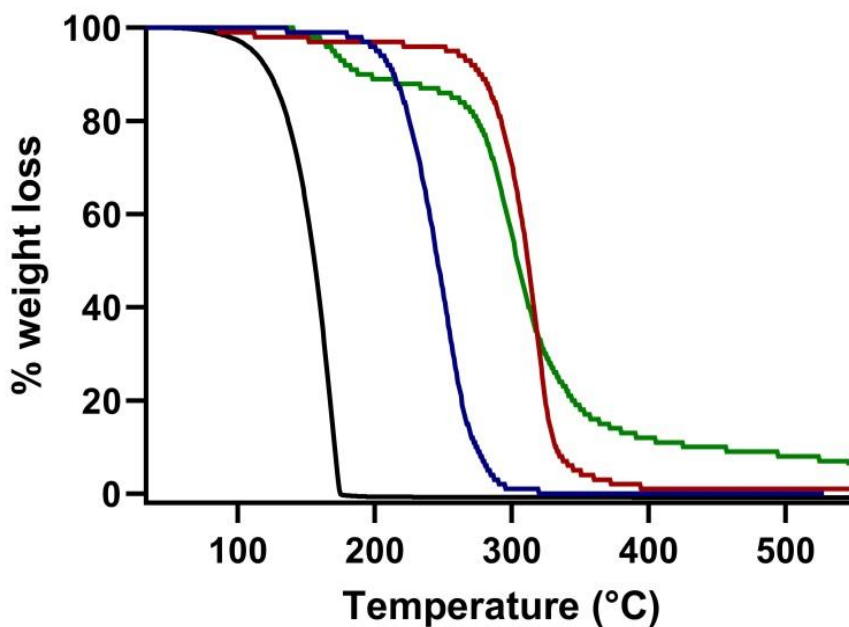


Figure S9 TGA analyses. Comparison between the results obtained for FJD₁, FJD₂ and FJD₃ and their fluorinated precursor F₂₇-N₃. Colour code: F₂₇-N₃ = black, FJD₁ = blue, FJD₂ = red, FJD₃ = green.

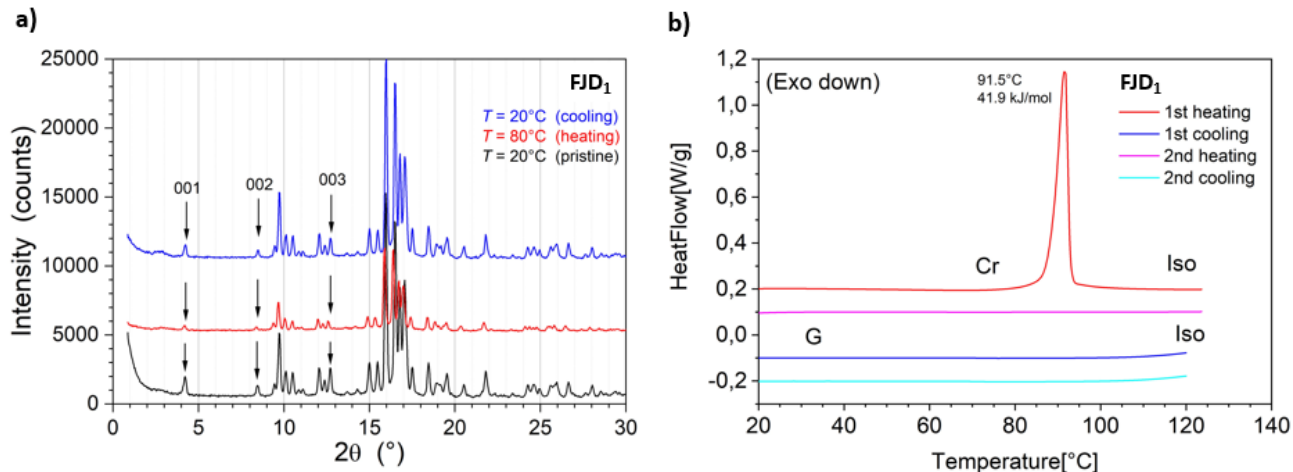


Figure S10 FJD₁ characterization in bulk. **a)** SWAXS diffractogram obtained at 20 °C (pristine state, black), at 80 °C (heating, red), and at 20 °C (on cooling, blue). **b)** DSC results: the first cycle shows a high energetic endothermic transition from a crystalline phase (Cr) to isotropic liquid phase (Iso), which was not observed on cooling (II cycle) and on further heating (III cycle). The solid phase is amorphous (G: glassy).

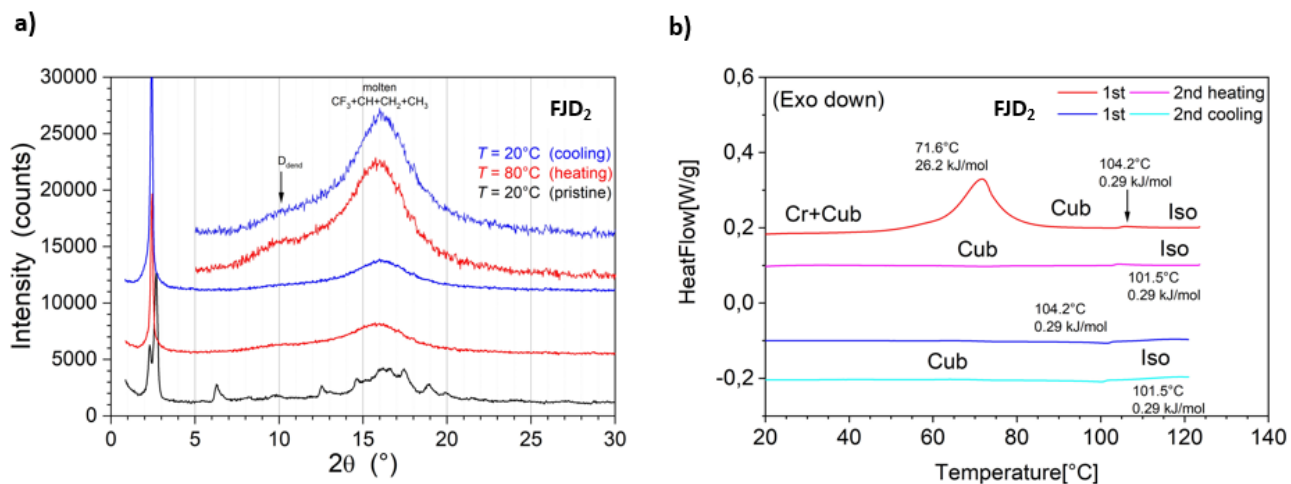


Figure S11 FJD₂ characterization in bulk. **a)** SWAXS analyses of FJD₂ in the pristine state at 20 °C (black), at 80 °C (red) and on cooling at 20 °C (blue). In the upper region of the graph red and blue curves are magnified to focus on peaks related to dimensions of the molecule (molten CF₃ and average dendrimer dimension, D_{dend}). **b)** DSC results. The first heating cycle (in red) show the transition from the pristine solid state to a reversible liquid crystalline mesophase (Cub), as confirmed in the second cycle (violet and light blue curves).

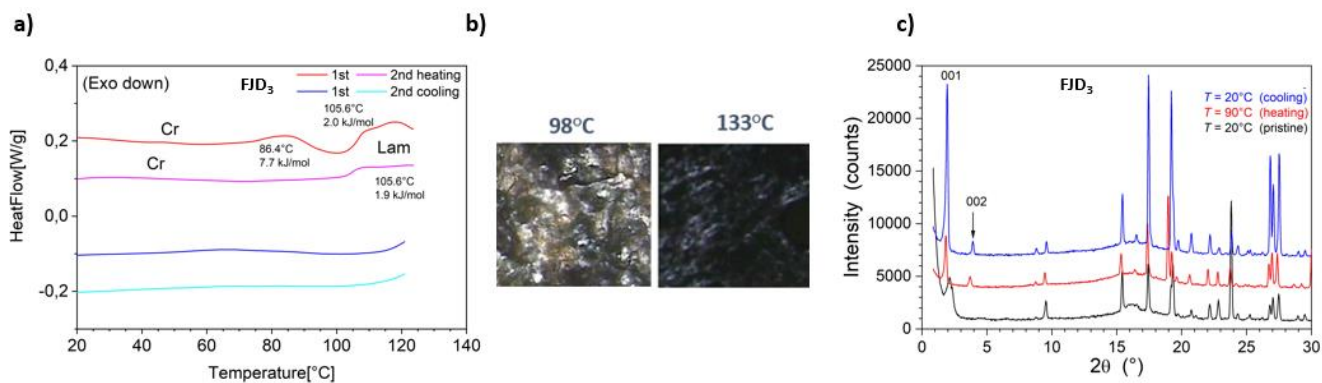


Figure S12 FJD₃ characterization in bulk. **a)** DSC results. First cycle: heating (red) and cooling (blue); second cycle: heating (violet) and second cooling (light blue). **b)** POM images: at 98 °C a partial melting occurs; at 133 °C birefringence was observed: the pattern suggests a lamellar LC phase. **c)** SWAXS analyses of FJD₃ in the pristine state at 20 °C (black), at 90 °C (red) and on cooling at 20 °C (blue).

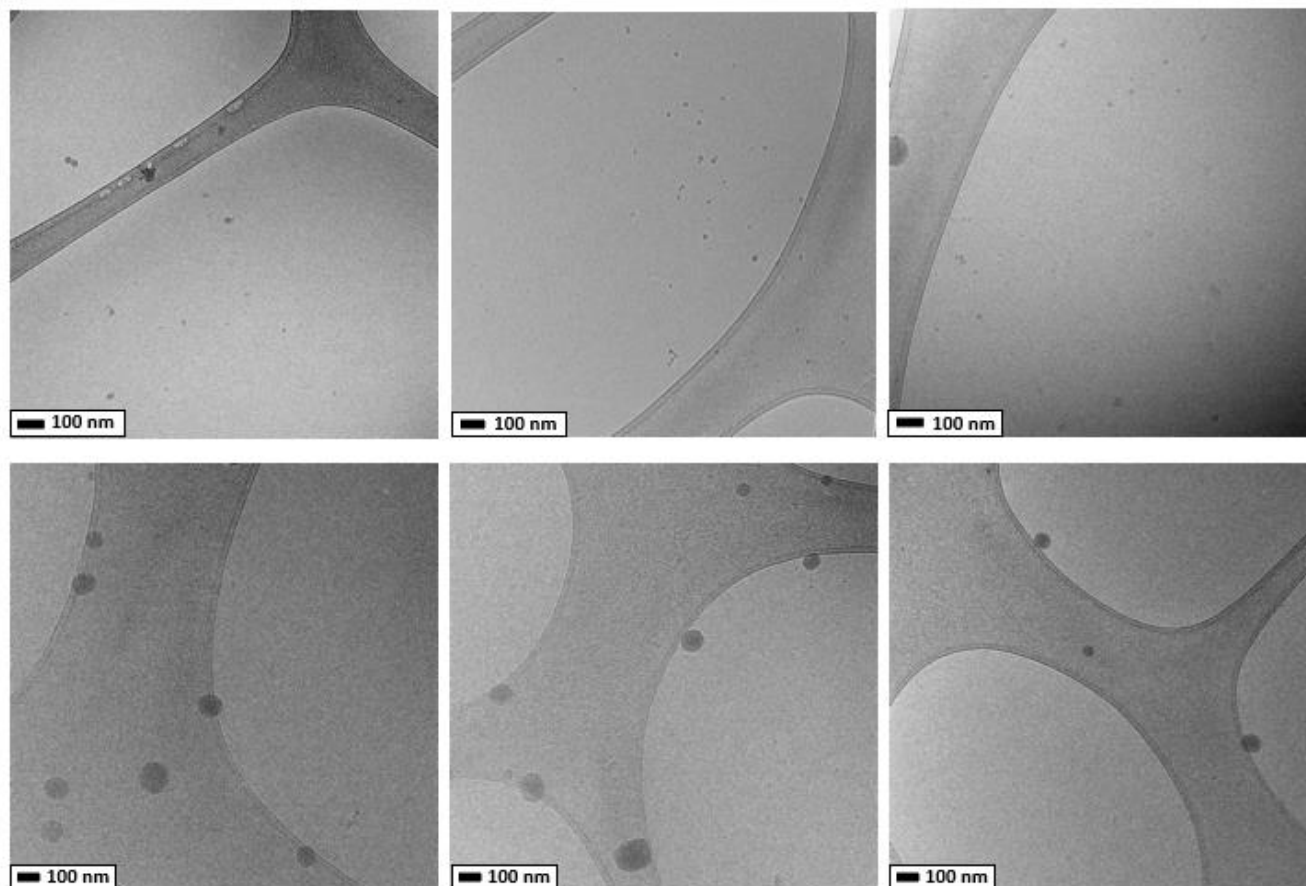


Figure S13 The ethanol in water procedure. Cryo-TEM images of the FJD₁ dispersions. Images highlighted the presence of two family of aggregates: micelles and larger spherical nanoparticles (100 nm diameter).

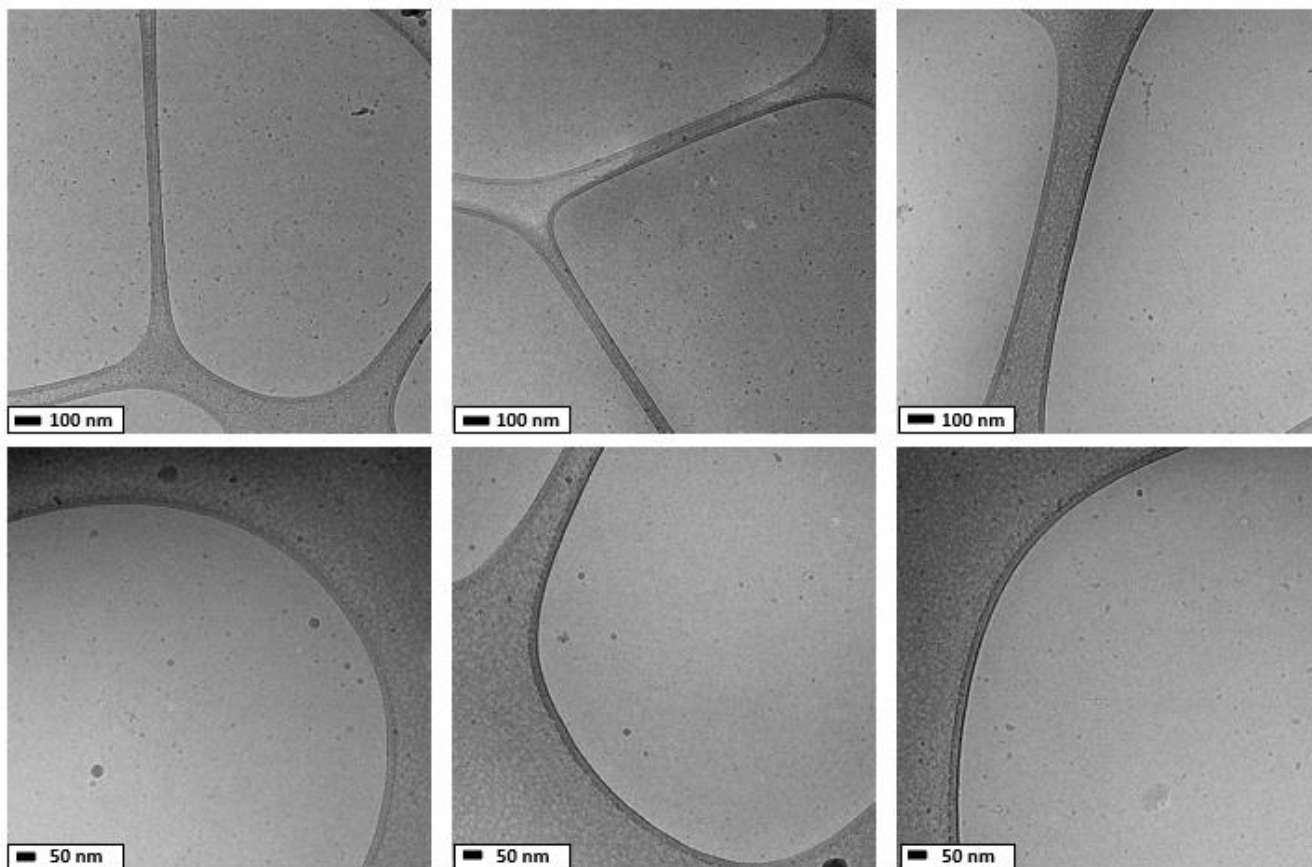


Figure S14 The ethanol in water procedure. Cryo-TEM images of the FJD₂ dispersions. Images highlighted the presence of two family of aggregates: micelles and larger spherical nanoparticles (50 nm diameter).

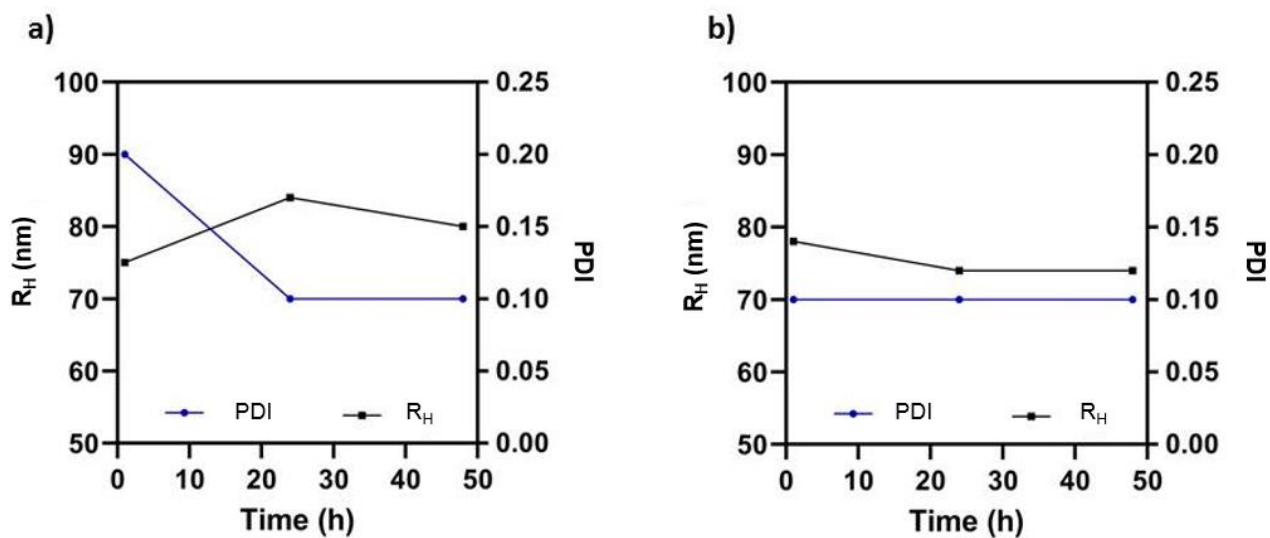


Figure S15 DSL results. **a)** FJD₁: changes in the hydrodynamic radius (R_H, blue) and polydispersity (PDI, black) overtime; **b)** FJD₂: changes in the hydrodynamic radius (R_H, blue) and polydispersity (PDI, black) overtime.

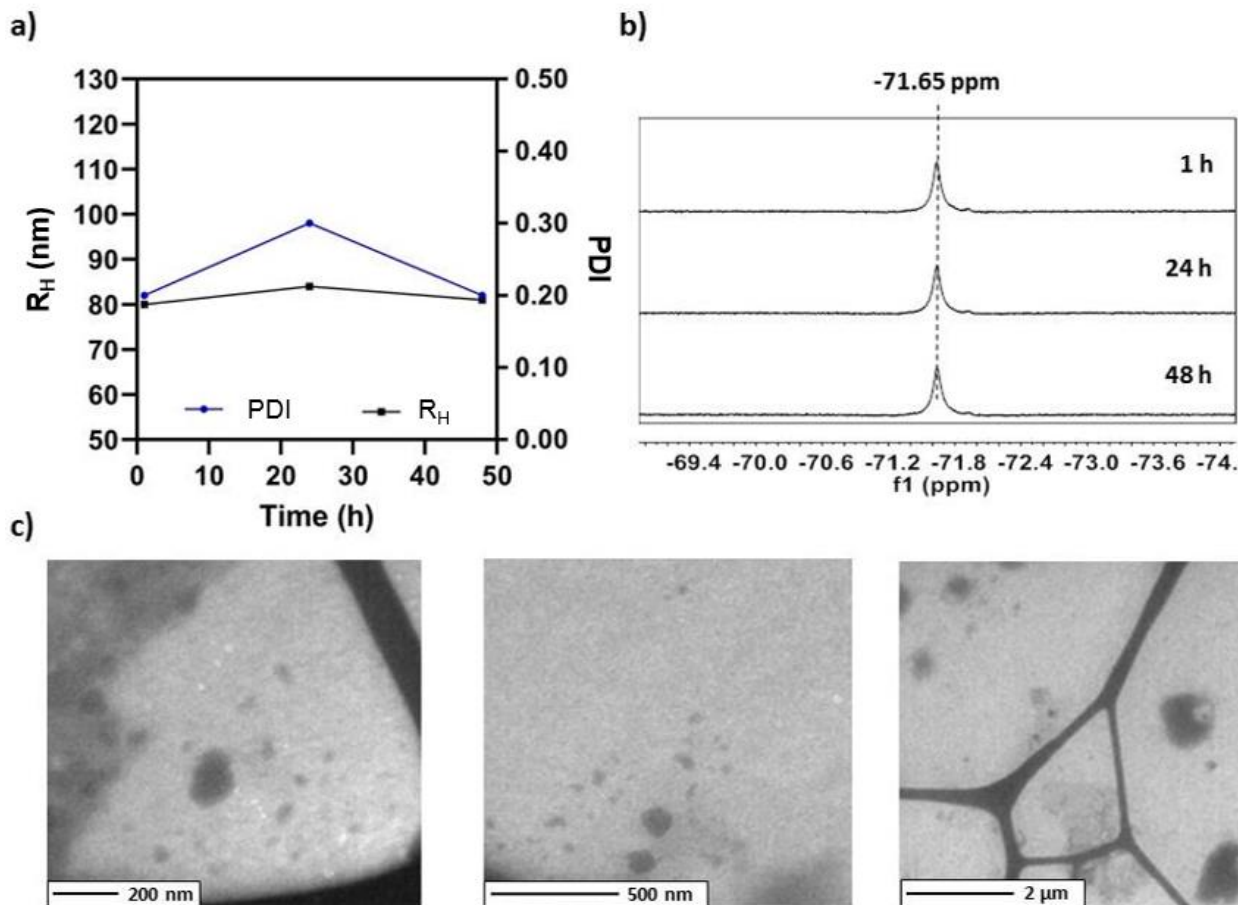


Figure S16 FJD₃ 0.3 mM self-assembly in water in presence of trifluoroethanol (TFE, $\delta = -76.6$ ppm) as cosolvent. **a)** DLS results. Changes in the hydrodynamic radius (R_H , blue) and polydispersity (PDI, black) overtime; **b)** ^{19}F -NMR of FJD₃ 0.3 mM overtime. Solvent: solution + D₂O (10% v/v). **c)** TEM images after 48 h from sample preparation. The absence of fibers, together with the stability observed at DLS and ^{19}F -NMR suggest that no transitions have occurred during sample ageing.

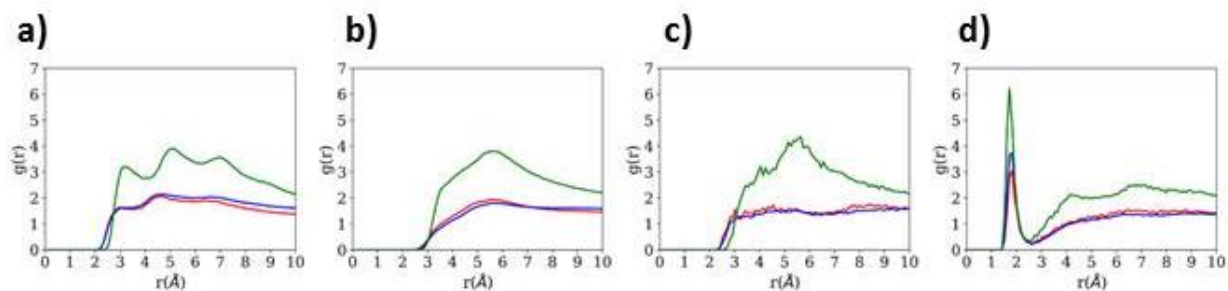


Figure S17 AA-MD simulations of a single FJD₃ molecule. Summary of results in four solvent conditions; water (black line), 5% of ethanol in water (red line), 25% of ethanol in water (blue line), 5% of TFE in water (green line): **a)** distances between fluorine atoms of the dendrimer and the terminal hydrogen atoms of ethanol or the fluorine atoms of TFE; **b)** distances between the sp^3 carbon atoms of the dendrimer and sp^3 carbon atoms of ethanol/TFE; **c)** distances between the nitrogen atoms of the dendrimer and the ethanol/TFE sp^3 carbons; **d)** distances between the carbonyl oxygens of the dendrimer and the hydrogens of the OH groups of ethanol/TFE.

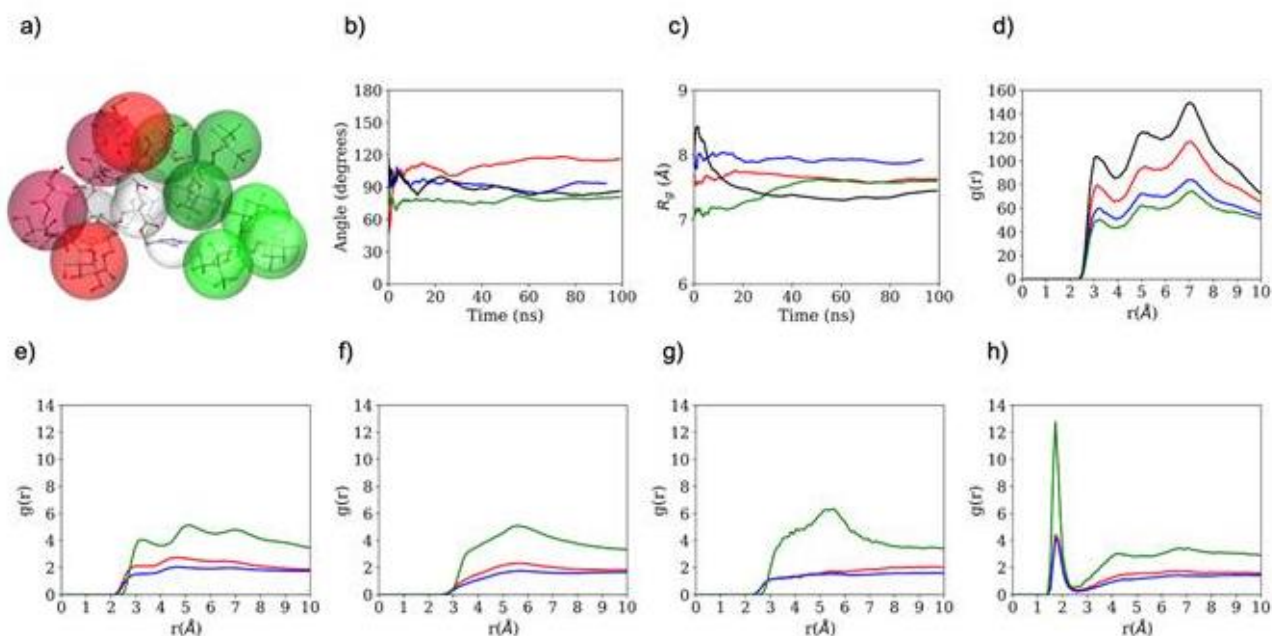


Figure S18 AA-MD simulations of two FJD₃ molecules in 4 solvents, pure water (black line), 5% of ethanol in water (red line), 25% of ethanol in water (blue line), 5% of TFE in water (green line):. a) a representative snapshot of the dynamics: hydrophilic moieties highlighted in red, fluorinated fragments in green, core in white; one molecule is in a darker representation to assist the eye; b) central dihedral angle of FJD₃ in time; c) R_g in time; RDF's d) the two dendrimers perfecta-fluorine atoms; e) distances fluorine atoms of the two dendrimers and the terminal hydrogen atoms of ethanol or the fluorine atoms of TFE f) distances between the sp^3 carbon atoms of the two dendrimers and sp^3 carbon atoms of ethanol/TFE; g) distances between the nitrogen atoms of the two dendrimers and the ethanol/TFE sp^3 carbons; h) distances between carbonyl oxygens of the two dendrimers and the hydrogens of the OH groups of ethanol/TFE.

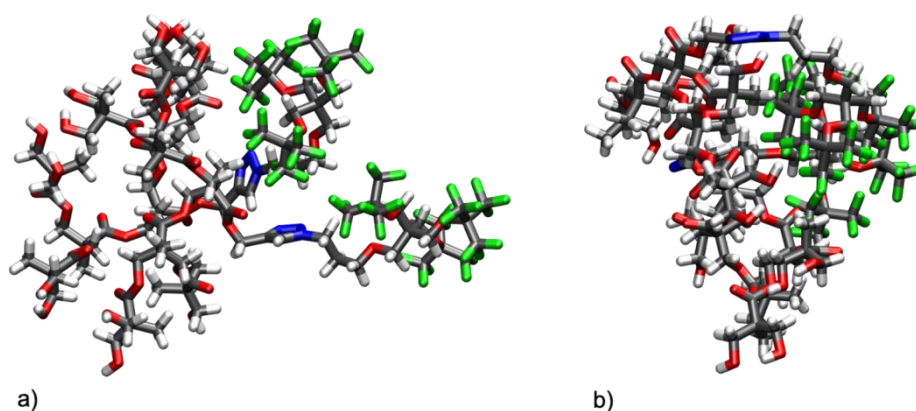


Figure S19 Representative FJD₃ structures of a) trans and b) cis conformations of dimer, where fluorine atoms are in green, carbon atoms in grey, oxygens in red, hydrogens in white and nitrogens in blue.

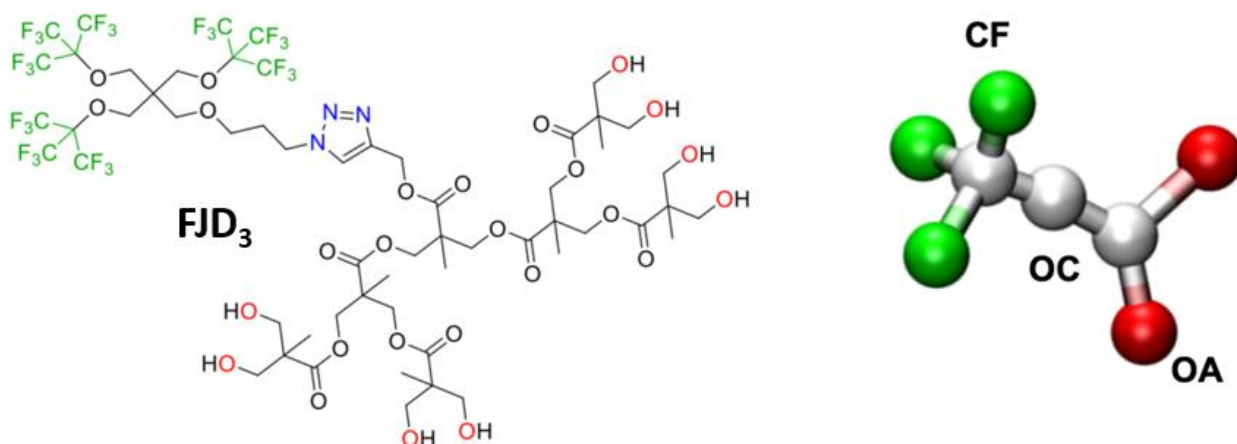


Figure S20 Molecular structure of FJD₃ (on the left) and the corresponding CG model implemented in our DPD simulations (on the right) where green beads represent the hydrophobic fluorinated groups (CF), the red beads the hydrophilic branched groups (OA) and the white bead a generic ether molecular group (OC) present in the region linking the terminal parts.

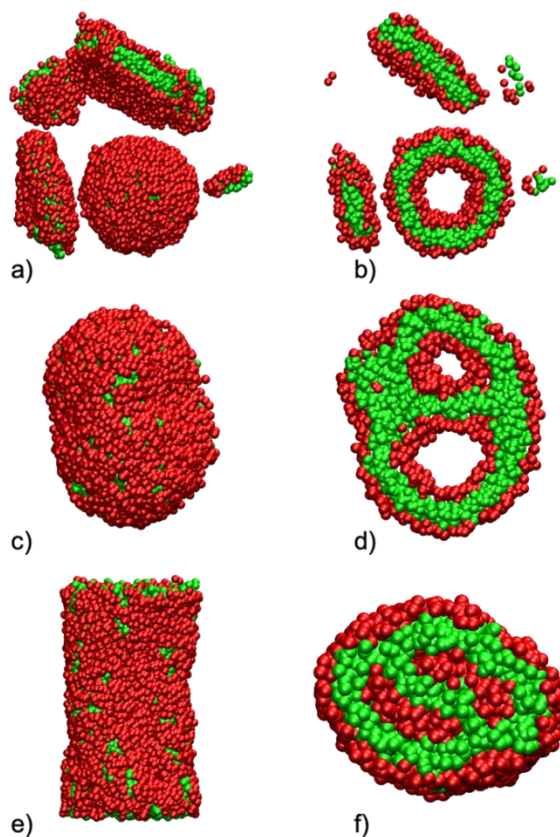


Figure S21 Snapshots of morphologies and corresponding cross sections of the inner core of aggregates obtained with different a_{OAS} parameters: a) and b) $a_{OAS} = 20$, c) and d) $a_{OAS} = 30$ and e) and f) $a_{OAS} = 35$. Simulation box of dimensions $40rc \times 40rc \times 40rc$. Colour code: hydrophilic groups in red; and hydrophobic groups in green. Water and OC beads are not represented here for sake of clarity.

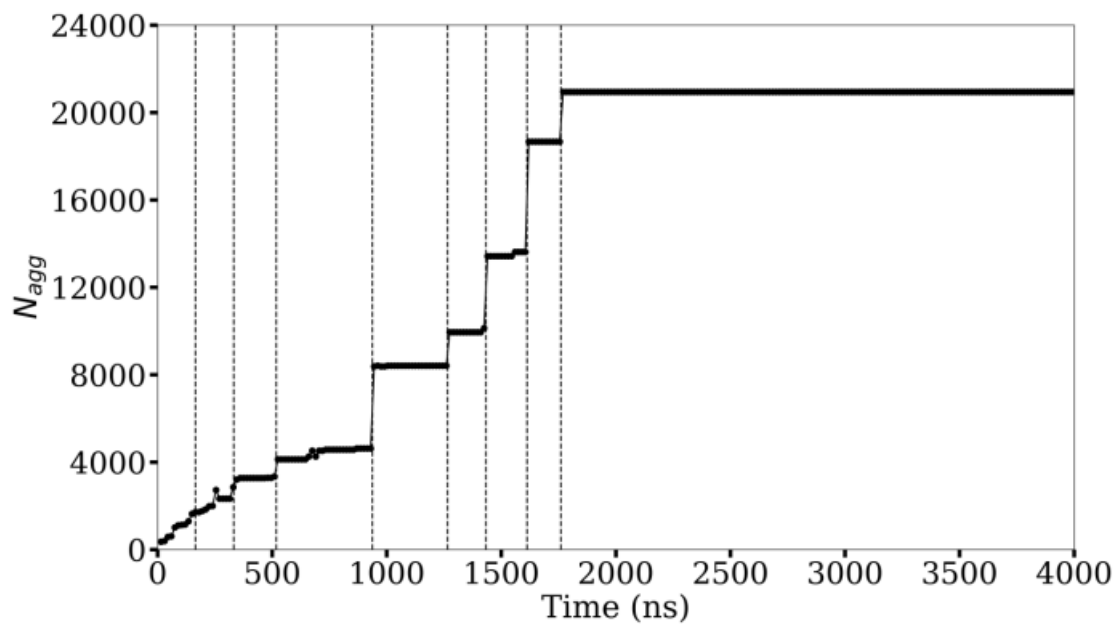


Figure S22 Time-dependent mean aggregation number in the first 4000 ns of the simulations run in water with $a_{OAS} = 30$ in the 80rc x 80rc x 80rc box. Vertical bars represent simulation steps where aggregation number abruptly increases.

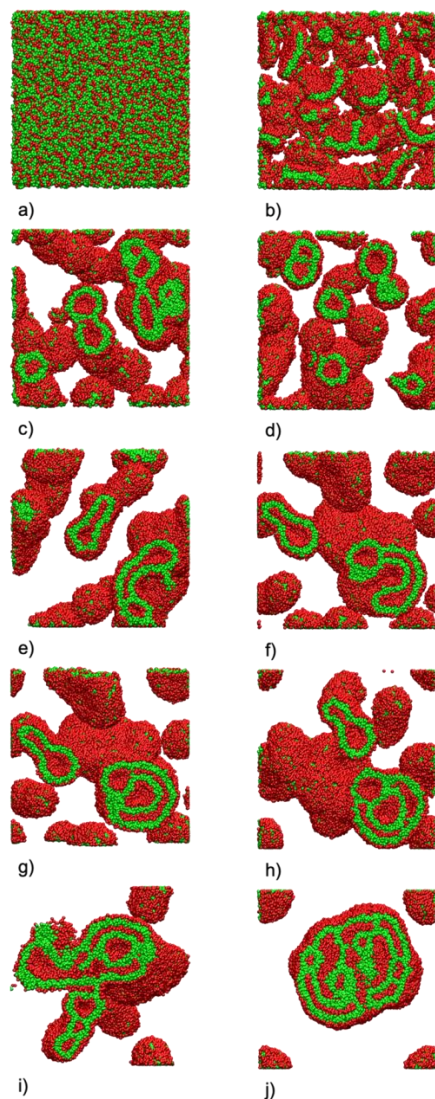


Figure S23 Snapshots of the morphology of aggregation obtained with $a_{OA,S}=30$ at different times, starting from a random configuration composed of 24,000 amphiphiles: a) $0 \mu s$, b) $0.165 \mu s$, c) $0.332 \mu s$, d) $0.518 \mu s$, e) $0.937 \mu s$, f) $1.265 \mu s$, g) $1.533 \mu s$, h) $1.612 \mu s$, i) $1.760 \mu s$, j) $4.200 \mu s$. Simulation box of dimensions $80r_c \times 80r_c \times 80r_c$. Colour code: hydrophilic groups in red; and hydrophobic groups in green. Water and OC beads are not shown to assist the eye.

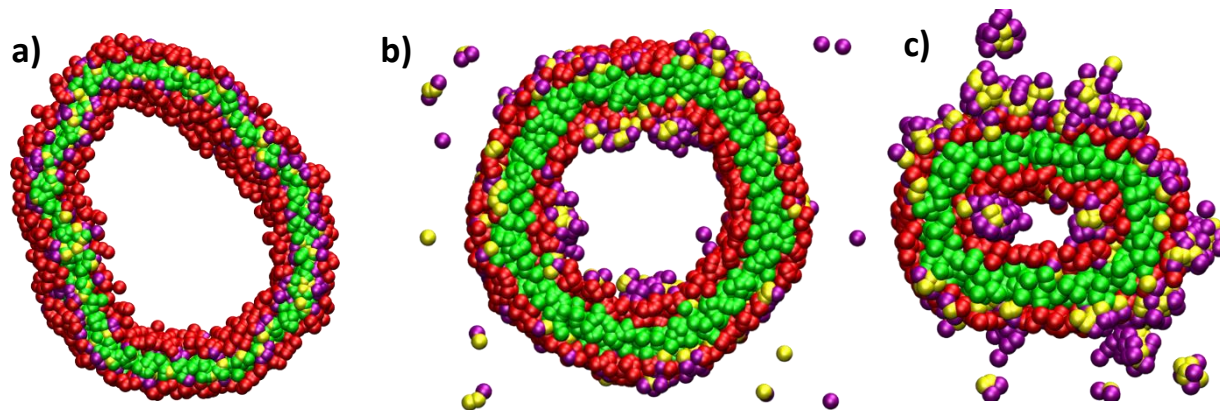


Figure S24 a) Snapshot of the cross section morphology obtained with TFE, also showing co-solvent beads. Colour code: dendrimer hydrophilic groups in red and dendrimer hydrophobic groups in green; co-solvent hydrophilic beads in violet, co-solvent hydrophobic beads in yellow. OC and water beads are not represented to assist the eye; b) Snapshot of the cross section morphology obtained at the lowest ethanol concentration, also showing co-solvent beads. Colour code: dendrimer hydrophilic groups in red and dendrimer hydrophobic groups in green; co-solvent hydrophilic beads in violet, co-solvent hydrophobic beads in yellow. OC and water beads are not represented to assist the eye; c) Snapshot of the cross section morphology obtained at the highest ethanol concentration, also showing co-solvent beads. Colour code: dendrimer hydrophilic groups in red and dendrimer hydrophobic groups in green; co-solvent hydrophilic beads in violet, co-solvent hydrophobic beads in yellow. OC and water beads are not represented to assist the eye.

- [1S] Martinez Espinoza M. I., Sori L., Pizzi A., Terraneo G., Moggio I., Arias E., Pozzi G., Orlandi S., Dichiarante V., Metrangolo P., Cavazzini M., Baldelli Bombelli F. (2019), BODIPY Dyes Bearing Multibranching Fluorinated Chains: Synthesis, Structural, and Spectroscopic Studies *Chemistry – A European Journal*, 25, 9078-9087.
- [2S] Yue X., Taraban M. B., Hyland L. L., Yu Y. B. (2012), Avoiding Steric Congestion in Dendrimer Growth through Proportionate Branching: A Twist on da Vinci's Rule of Tree Branching, *Journal Organic Chemistry*, 77, 8879–8887.
- [3S] Lausi A., Polentarutti M., Onesti S., Plaisier J. R., Busetto E., Bais G., Barba L., Cassetta A., Campi G., Lamba D., Pifferi A., Mande S. C., Sarma D. D., Sharma S. M., Paolucci G. (2015). Status of the crystallography beamlines at Elettra. *The European Physical Journal Plus*, 130(43), 1-8.
- [4S] Kabsch W. (2010). XDS. *Acta Crystallographica Section D*, 66(2), 125–132.
- [5S] Winn, M. D., Ballard, C. C., Cowtan, K. D., Dodson, E. J., Emsley, P., Evans, P. R., Keegan, R. M., Krissinel, E. B., Leslie, A. G. W., McCoy, A., McNicholas, S. J., Murshudov, G. N., Pannu, N. S., Potterton, E. A., Powell, H. R., Read, R. J., Vagin, A. & Wilson, K. S. (2011). Overview of the CCP4 suite and current developments. *Acta Crystallographica Section D*. 67, 235-242.
- [6S] Evans P. R. and Murshudov G. N. How good are my data and what is the resolution?. (2013). *Acta Crystallographica Section D*. 69, 1204-1214
- [7S] Sheldrick G. M. (2015). SHELXT – Integrated space-group and crystal-structure determination. *Acta Crystallographica Section A*, 71, 3-8.
- [8S] Sheldrick G. M. (2015). Crystal structure refinement with SHELXL. *Acta Crystallographica Section C*, 71, 3-8.
- [9S] Emsley P., Lohkamp B., Scott W.G., Cowtan K. (2010). Features and development of Coot. *Acta Crystallographica Section D*, 66(4), 486–501.
- [10S] Macrae, C. F., Sovago I., Cottrell S. J., Galek P. T. A., McCabe P., Pidcock E., Platings M., Shields G. P., Stevens J. S., Towler M., Wood P. A. (2020). Mercury 4.0: from visualization to analysis, design and prediction. *Journal of Applied Crystallography* 53(1), 226-235.